

# Material Matters™

VOLUME 12 • NUMBER 2

## Connecting the Dots

### Tools for Drug and Gene Delivery

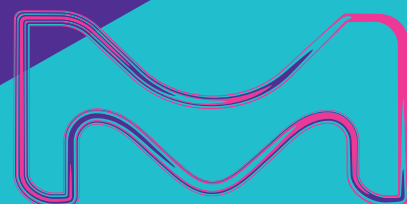
**BIODEGRADABLE ALIPHATIC POLYESTERS** for Drug Delivery

**POLYMERSOMES** for Drug Delivery

**PROTEIN- AND PEPTIDE-POLYMER CONJUGATES** by RAFT Polymerization

**FUNCTIONALIZED PEI** and Its Role in Gene Therapy

**COLLAGEN** in Gene Delivery Applications



## Introduction



**Brianna Upton, Ph.D.**

Product Manager,  
Biomedical Materials

Welcome to the second issue of *Material Matters*™ for 2017, focused on novel polymer materials and techniques for drug and gene delivery research. This issue highlights new and innovative synthetic and natural materials and methods for solving critical issues in the development of new drug delivery methods.

In the first article, Professor Mihaela Stefan (University of Texas at Dallas, USA) discusses the synthesis and application of aliphatic polyesters commonly used in drug delivery systems. The resulting material properties, such as degradation or self-assembly, can be directly controlled through the selection of monomer identity and polymer structure.

As synthetic analogs to liposomes, polymersomes offer great promise in drug delivery applications. In the second article, Professor Luke Connal (University of Melbourne, Australia) outlines applications and strategies for utilizing polymersomes in controlled release and targeted drug delivery applications.

In the third article, Professor Sébastien Perrier (University of Warwick, UK and Monash University, Australia) highlights the strengths of reversible addition-fragmentation chain transfer (RAFT) polymerization as a method for the synthesis of polymer-biomolecule conjugates. By combining the strengths of synthetic polymers and biomolecules, a novel class of advanced biomaterials with enhanced properties can be obtained for use in drug delivery applications.

Due to its ability to readily form polyplexes with nucleic acids, poly(ethyleneimine) (PEI) has been extensively explored as a carrier for gene delivery. Despite its strengths, PEI has been shown to aggregate in the blood, leading to high cytotoxicity in both *in vitro* and *in vivo* applications. In the fourth article, Professor Olivia Merkel (Ludwig-Maximilians-Universität München, Germany) highlights recent advances in the development of PEI derivatives as gene carriers for small interfering RNA (siRNA) and DNA.

While collagen is most commonly used as a structural scaffold, it can also be used as a reservoir for the retention and delivery of signaling molecules or genes. In the fifth article, Professors Kristi L. Kiick and Millicent O. Sullivan (University of Delaware, USA) discuss collagen as a highly-tunable and promising biomaterial for gene delivery applications.

In this issue, each article is accompanied by a list of polymers and related products available from our portfolio. For additional product information, visit us at [SigmaAldrich.com/matsci](http://SigmaAldrich.com/matsci). As always, please bother us with your new product suggestions as well as thoughts and comments for *Material Matters*™ at [matsci@sial.com](mailto:matsci@sial.com), to help us continue to grow our polymer offering.

## Welcome to the Future of *Material Matters*™



**Bryce P. Nelson, Ph.D.**  
Materials Science  
Initiative Lead

Welcome to the new look of *Material Matters*™. Over its 12-year history, *Material Matters*™ has consistently brought you reviews of the latest in materials science as well as information on new products for research. As part of the Merck KGaA, Darmstadt, Germany family, we're proud to grow as a company and better serve our customers. While you'll notice an evolution in the design of *Material Matters*™, the fundamental quality and trust that made Aldrich and

Sigma-Aldrich a part of laboratories worldwide remains intact. We are confident that you will continue to find unique benefit in our scientists and collaborators for many years in the future.

We have a new look and the same great articles. We continue to bring you the latest ideas and products to help drive your research. As always, previous issues of *Material Matters*™ are available online at [SigmaAldrich.com/mm](http://SigmaAldrich.com/mm).

Merck KGaA, Darmstadt, Germany  
Frankfurter Strasse 250  
64293 Darmstadt, Germany  
Phone +49 6151 72 0

### To Place Orders / Customer Service

Contact your local office or visit  
[SigmaAldrich.com/order](http://SigmaAldrich.com/order)

### Technical Service

Contact your local office or visit  
[SigmaAldrich.com/techinfo](http://SigmaAldrich.com/techinfo)

### General Correspondence

Materials Science  
[materialsscience@sial.com](mailto:materialsscience@sial.com)

### Subscriptions

Request your FREE subscription to *Material Matters*™ at [SigmaAldrich.com/mm](http://SigmaAldrich.com/mm)

The entire *Material Matters*™ archive is available at [SigmaAldrich.com/mm](http://SigmaAldrich.com/mm)

*Material Matters*™ (ISSN 1933-9631) is a publication of Merck KGaA, Darmstadt, Germany

Copyright © 2017 EMD Millipore Corporation. All Rights Reserved. MilliporeSigma and the Vibrant M are trademarks of Merck KGaA, Darmstadt, Germany. *Material Matters*, Sigma-Aldrich, Supelco, SAFC and Bioreliance are trademarks of SigmaAldrich Co. LLC, or its affiliates. All other trademarks are the property of their respective owners. Purchaser must determine the suitability of the products for their particular use. Additional terms and conditions may apply. Please see product information on the Sigma-Aldrich website at [SigmaAldrich.com](http://SigmaAldrich.com) and/or on the reverse side of the invoice or packing slip.

# Table of Contents

## Articles

Biodegradable Aliphatic Polyesters for Drug Delivery	37
Polymersomes for Drug Delivery	45
Protein- and Peptide-Polymer Conjugates by RAFT Polymerization	53
Functionalized PEI and Its Role in Gene Therapy	63
Collagen in Gene Delivery Applications	68

## Featured Products

Biodegradable Aliphatic Polyesters A selection of dioxanone, $\epsilon$ -caprolactone, glycolide, lactide-based copolymers, and functionalized polymers	41
Amphiphilic Block Copolymers A selection of PS-PAA, PS-PMMA, PS-PEG, and PS-PAA copolymers	50
Biodegradable Amphiphilic Block Copolymers A selection of biodegradable PEG-PLA, PEG-PLGA, PEG-PCL, PLA-PAA, and PLA-co-MAC materials	51
RAFT Agents A selection of trithiocarbonate, dithiocarbonate, and dithiobenzoate RAFT agents	59
Macro-RAFT Agents A selection of PEG, PS, PLA, and PAA based materials	61
Poly(ethyleneimine) A selection of linear, branched, and functionalized PEIs	67
High-Purity Collagen A selection of high-purity collagen materials	75

## About the Cover

Advances in pharmaceutical and gene technology require new techniques to deliver a therapeutic in the right quantity and to the right location. As the pace of drug discovery increases, polymeric materials for drug and gene delivery must also evolve to create new pharmaceutical solutions. This issue's cover art illustrates the connection and interplay between each component of a drug or gene delivery system for successful translation to the patient.

## Your Material Matters



*Ken Yoon*

Ken Yoon, Ph.D.  
Head of Lab and Specialty Chemicals

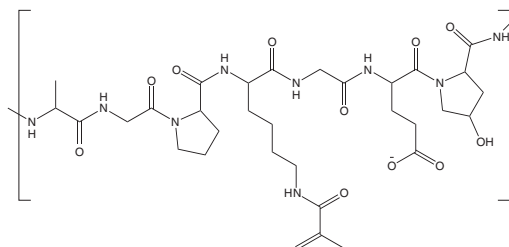
We welcome fresh product ideas. Do you have a material or compound you wish to see featured in our Materials Science line? If it is needed to accelerate your research, it matters. Send your suggestion to [matsci@sial.com](mailto:matsci@sial.com) for consideration.

Professor Ali Khademhosseini at Harvard-MIT Division of Health Sciences and Technology, USA, recommended the addition of gelatin methacryloyl (Prod. No. **900496**) to our catalog for use in tissue engineering applications. Gelatin methacryloyl is a versatile material that can be combined with PEG,<sup>1,2</sup> carbon nanotubes,<sup>2</sup> or many other materials to create composite hydrogel platforms with desired features, such as enzymatic degradability and tunable mechanical and biological properties. Several studies also report the use of photopolymerizable gelatin methacryloyl in 3D bioprinting,<sup>4,7</sup> to support formation of functional vascular networks,<sup>6</sup> endothelial cell morphogenesis,<sup>8</sup> and cardiomyocyte alignment.<sup>9</sup> Gelatin methacryloyl has also been explored in drug delivery applications in the form of microspheres<sup>10,11</sup> and hydrogels.<sup>12</sup>

## References

- Hutson, C. B.; Nichol, J. W.; Aubin, H.; Bae, H.; Yamanlar, S.; Al-Ahque, S.; Koshy, S. T.; Khademhosseini, A. *Tissue Eng. Part A*. **2011**, *17*(13-14), 1713.
- Nichol, J. W.; Koshy, S. T.; Bae, H.; Yamanlar, S.; Khademhosseini, A. *Biomaterials*. **2010**, *31*(21), 5536.
- Shin, S. R. et al. *ACS Nano*. **2013**, *7*(3), 2369.
- Bertassoni L.E. et al. *Biofabrication*. **2014**, *6*, 024105.
- Billiet, T.; Gevaert, E.; De Schryver, T.; Cornelissen, M.; Dubruel, P. *Biomaterials*. **2014**, *35*(1), 49-62.
- Skardal, A.; Zhang, J.; McCoard, L.; Xu, X.; Oottamasathien, S.; Prestwich, G. D. *Tissue Eng. Part A*. **2010**, *16*(8), 2675-85.
- Boere K.W. et al. *Acta Biomater*. **2014**, *10*(6), 2602.
- Nikkhah, M. et al. *Biomaterials*. **2012**, *33*(35), 9009.
- Tsang K.M.C. et al. *Adv. Funct. Mater*. **2015**, *25*(6), 977-86.
- Cha, C. et al. *Biomacromolecules*. **2014**, *15*, 283.
- Nguyen, A. H.; McKinney, J.; Miller, T.; Bongiorno, T.; McDevitt, T. C. *Acta Biomater*. **2015**, *13*, 101.
- Gupta, N. V.; Satish, C. S.; Shivakumar, H. G. *Indian J. Pharm. Sci*. **2007**, *69*(1), 64.

## Gelatin methacryloyl



Gelatin methacryloyl, 80% degree of substitution  
powder

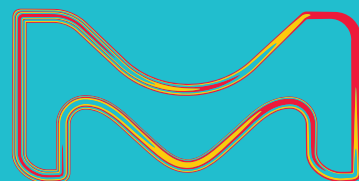
store at 2-8 °C

**900496-1G**

1 g

**Sigma-Aldrich®**

Lab Materials & Supplies

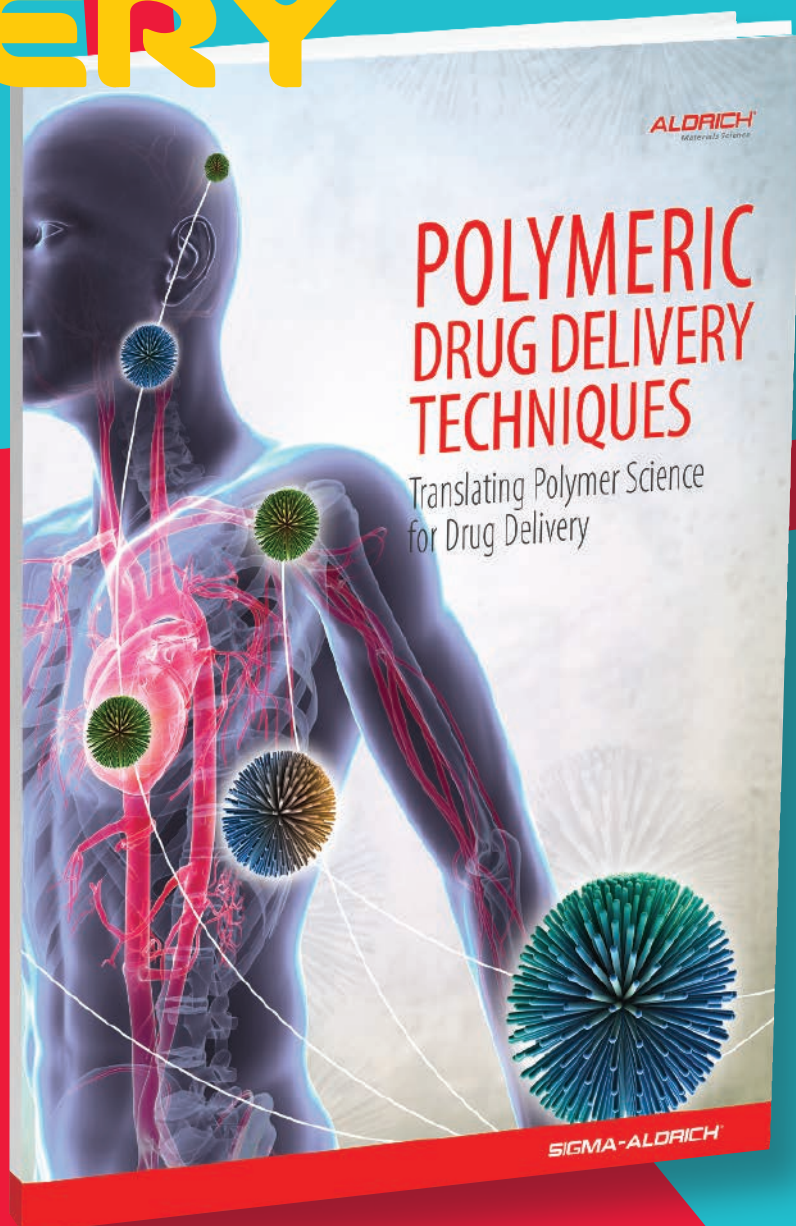


# IMPROVE DELIVERY

## A Step-by-Step Guide

Low drug solubility and stability often reduce the effectiveness of an otherwise promising therapeutic candidate. In this comprehensive guide, you'll discover how polymers can provide the drug delivery solutions you need for controlled release, targeting, and solubility enhancement.

Request your copy online at:  
[SigmaAldrich.com/ddtechnique](http://SigmaAldrich.com/ddtechnique)



The life science business of Merck KGaA, Darmstadt, Germany operates as MilliporeSigma in the U.S. and Canada.

**Millipore  
SIGMA**

# Biodegradable Aliphatic Polyesters for Drug Delivery



Vasanthy Karmegam,<sup>1</sup> Pooneh Soltantabar,<sup>2</sup> Erika Joy L. Calubaquib,<sup>1</sup> Ruvanathi N. Kularatne,<sup>1</sup> Mihaela C. Stefan<sup>1,2\*</sup>

<sup>1</sup>Department of Chemistry and Biochemistry, University of Texas at Dallas, Richardson, TX 75080

<sup>2</sup>Department of Bioengineering, University of Texas at Dallas, Richardson, TX 75080

\*Email: mihaela@utdallas.edu

## Introduction

Innovations in polymer technology have had a significant impact on the advancement of novel drug delivery systems. Most polymer-based drug delivery systems are designed to deliver a large dose of a therapeutic agent at a targeted site in a controlled manner, to reduce dosage frequency. However, the accumulation of polymer-based drug carriers in the body can pose a significant health risk and represents a major disadvantage of many polymer-based drug delivery systems. For example, the poor biodegradability of polystyrene (PS), poly(methyl methacrylate) (PMMA), and poly(*N*-isopropylacrylamide) (PNIPAM) have limited their potential applicability in drug delivery applications.<sup>1</sup>

In contrast, aliphatic polyesters have gained significant traction in recent decades as drug delivery systems due to their biodegradability and biocompatibility. The degradation of the polyester backbone *in vivo* prevents accumulation of the carrier material and degraded products in the body, reducing the risk of long-term toxicity.<sup>2</sup> Common polyesters used in drug delivery applications include poly(lactide)s (PLA), poly(caprolactone)s (PCL), poly(glycolide)s (PGA), poly(dioxanone)s (PDO), poly(butyrolactone)s (PBL), poly(valerolactone)s (PVL), and poly(lactide-co-glycolide) (PLGA) (Figure 1).<sup>3</sup>

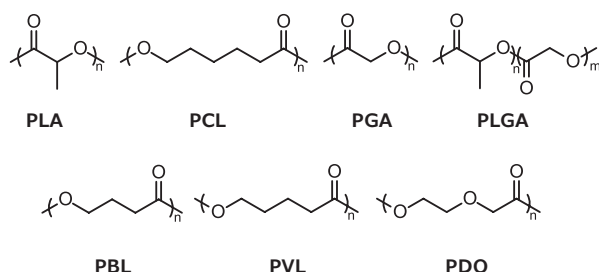


**Figure 1.** Polyesters commonly used in drug delivery applications.

A significant focus of current cancer therapy research is the delivery of anti-cancer drugs to tumor sites in a targeted manner, combined with activated release of the therapeutic payload. Stimuli-responsive polymeric drug carriers typically utilize nanocarriers (e.g., micellar systems, nanoparticles, polymersomes, or dendrimers) to release the drug at the tumor site by taking advantage of differences in the physiological environment between cancerous and healthy tissue. To further enhance the site-specificity of drug carriers, they can be conjugated with targeting moieties to allow for delivery at a specific tumor site. This article focuses on recent advances in the development of aliphatic polyesters for cancer therapy, specifically polyester synthesis, stimuli-responsive drug carriers, and active targeting.

## Polyester Synthesis

There are several strategies for the synthesis of aliphatic polyesters, including the polycondensation of diacids and diols as well as the ring-opening polymerization (ROP) of cyclic esters. Disadvantages of polycondensation include the requirements of accurate stoichiometry between reactants, continuous removal of by-products (e.g., water), high temperatures, long reaction times, and difficulty obtaining high molecular weight polymers.<sup>4</sup> In contrast, ring-opening polymerization typically results in high molecular weight polyesters and features limited side reactions. Based on its ease of use and the wide variety of initiators and catalysts available, ROP is widely used to polymerize cyclic ester monomers. The three most common mechanisms used in cyclic ester ring-opening polymerization are coordination-insertion, enzymatic, and anionic.<sup>4</sup>

Coordination-insertion ROP is initiated by an alcohol or amine and catalyzed by metal complexes based on Lewis acidic metals such as tin, aluminum, and zinc.<sup>1</sup> While this method yields high molecular weight polymers, residual traces of the metal catalyst in the final polymer have been considered a major drawback

limiting biological applications. For example, tin(II) bis(2-ethylhexanoate) (Prod. No. **S3252**), is an FDA-approved food additive commonly used for polyester synthesis, but due to the toxicity of tin, the residual concentration must remain below a certain threshold for use in food or biomedical applications.<sup>4</sup>

Enzymatic ROP commonly uses lipases as the catalyst in mild conditions, avoiding the use of toxic metals. While this method allows for the production of polyesters with stereo-, chemo- and regio-selectivity,<sup>5</sup> the resulting polyesters are commonly produced in relatively low yield with high polydispersity.<sup>3</sup> Anionic ROP yields high molecular weight polyesters but these reactions frequently undergo side reactions, due to backbiting.<sup>4</sup>

## Polyester Drug Carriers and Drug Release

Choosing an appropriate polymer vehicle and aptly tuning its properties ensures increased drug loading efficiency, reduction of drug dose and dosing frequency, alleviation of side effects, improvement of patient compliance, and short *in vivo* half-lives for drug delivery. Micelles, nanoparticles, and polymersomes are the most commonly explored drug carriers from synthetic polymers, formed by the self-assembly of amphiphilic block copolymers. Nanoparticle formation can be controlled kinetically through the variation of temperature, pH, electrolytes, and solvents and typically range in size from 10 to 1000 nm.<sup>3,7</sup> Micelle formation is thermodynamically controlled,<sup>6</sup> proceeding only when unimers aggregate above the critical micelle concentration (CMC), to form particles with sizes ranging from 5 to 100 nm.<sup>3,7</sup> Upon interaction with hydrophobic segments, a hydrophobic drug will migrate into the core of the micelle to form a core-shell matrix. In contrast, polymersomes are composed of a core filled with aqueous solution surrounded by a bilayer membrane composed of hydrophilic coronas located both on the inside and outside of the sphere. This unique structure enables polymersomes to encapsulate both hydrophobic and hydrophilic drugs.

Polymeric drug carriers facilitate the delivery of high drug payload to the site of action and allow controlled and sustained drug release under physiological conditions through erosion or stimuli-triggered release.<sup>2,3,8</sup> Upon water permeation, polyesters can undergo degradation via hydrolysis resulting in loss of polymer mass. Depending on the identity of the polymer backbone, erosion can either occur at the bulk or the surface of the nanocarrier (**Figure 2**). Surface erosion occurs when the rate of degradation is faster than the rate of water permeation into the bulk polymer. In contrast, bulk erosion occurs when water penetrates the bulk of the polymer at a faster rate than the erosion rate. The majority of biodegradable polyesters degrade via bulk erosion due to the increased ratio of aliphatic content. Recently, polymeric drug carriers with enhanced surface area have been utilized to control drug release, taking advantage of both surface and bulk erosion mechanisms.<sup>2,5,8</sup>

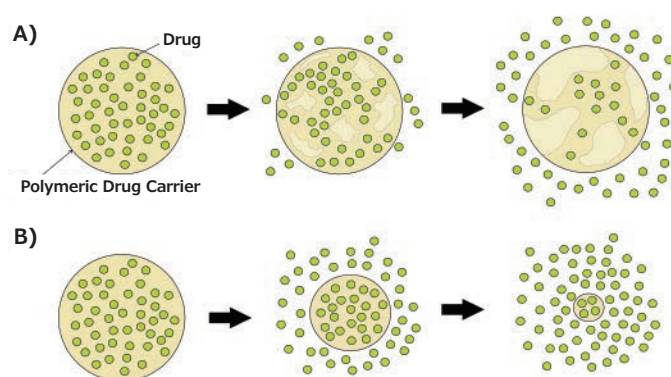


**Figure 2.** Degradation mechanisms of biodegradable polymeric drug carriers: A) bulk erosion, B) surface erosion.

Some carriers are designed to release the loaded drug only when exposed to external stimuli such as pH, temperature, reduction, enzymes, and light, preventing premature release of the encapsulated drug (**Figure 3**).<sup>3</sup> This results in an increased therapeutic efficacy of the drug and a decrease of potential toxicity to healthy cells.<sup>9</sup>

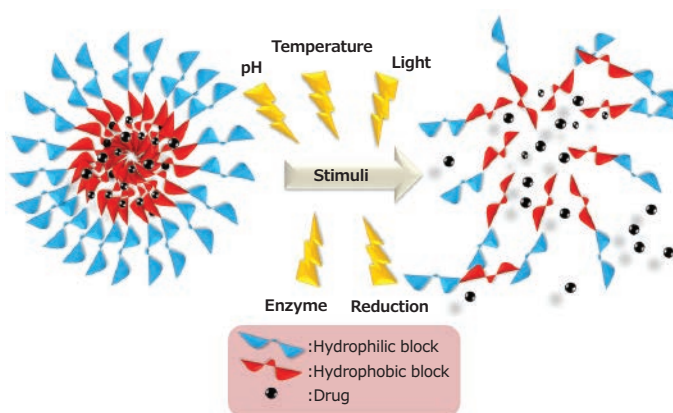


**Figure 3.** Schematic representation of stimuli-responsive drug release.

## Stimuli-Responsive Polyester Drug Carriers

Polymeric drug carriers are able to enter tumor sites through passive targeting via the enhanced permeability and retention (EPR) effect. As a result of this phenomenon, nanoparticles in the size range of 10 to 100 nm accumulate in tumor sites due to the presence of leaky vasculature.<sup>3</sup> In addition to utilizing this effect, polymeric drug carriers can be designed to respond either to a single or multiple stimuli by taking advantage of the difference in physiological environment between normal and tumor tissue. The difference in acidity between healthy and cancerous tissue allows for the development of pH-dependent release mechanisms.

For example, the pH of healthy tissue is 7.4 whereas the extracellular environment of the tumor tissue is 6.8 and intracellular endo/lysosomal pH is in the range of 4.0–6.5.<sup>10</sup> In the presence of acid-labile functional groups, drug carriers are cleaved in an acidic environment, releasing a drug at the tumor site. Synthesis of a pH-responsive (mPEG-PLA)-curcumin prodrug and further self-assembly into a micellar system was investigated by Zhao and coworkers.<sup>11</sup> The drug, which was conjugated to the polymer via a pH-responsive acetal linkage, showed more than 45% release at pH 5 after 48 hours while less than 20% of curcumin was released from the micellar system at pH 7.4.<sup>11</sup>

The difference in concentration of glutathione (GSH) between healthy cells and cancer cells can also be used as a stimulus. Tumor cells have an intracellular GSH concentration of ~2–10 mM, several times higher than the concentration in healthy cells.<sup>10</sup> The increased GSH concentration can cleave reduction-responsive disulfide bonds, allowing the release of the loaded cargo into the tumor site.<sup>12</sup> A reduction-responsive micellar drug delivery system based on disulfide bond-containing PEG-PLA amphiphilic block copolymers was developed by Shen and coworkers. In a reductive environment, the breaking of disulfide bonds caused the rapid release of doxorubicin (DOX). Up to 64% of DOX was released from PEG2000-PLA5000 micelles after 14 hours in the presence of the reducing agent dithiothreitol (DTT). In the absence of DTT, only 40% of DOX was released after 14 hours.<sup>12</sup>

Thermally responsive drug delivery systems typically consist of polymers featuring a lower critical solution temperature (LCST) and upper critical solution temperature (UCST). Above their LCST, the polymers undergo a phase transition, becoming insoluble in water.<sup>13</sup> Polymers with an LCST above normal physiological temperature (37 °C) are typically used in thermally responsive systems. These polymers are able to preserve their cargo in the body and undergo phase transition with the application of heat, leading to a burst release of drug in tumor tissue. A thermo-responsive monomer,  $\gamma$ -2-[2-(2-methoxyethoxy)ethoxy]ethoxy- $\epsilon$ -caprolactone (MEEECL), was introduced by Stefan et al. and combined with octyloxy- $\epsilon$ -caprolactone (OCTCL) to create an amphiphilic block copolymer with a LCST of 38 °C.<sup>14</sup> The LCST could be adjusted in the range of 31–43 °C by replacing OCTCL with  $\gamma$ -(2-methoxyethoxy)- $\epsilon$ -caprolactone (MECL). The size of the resulting micelles increased from approximately 150 nm to 400 nm when the temperature exceeded the LCST of copolymer.<sup>13</sup> Moreover, they demonstrated (experimentally and computationally) the effect of varying the substituent in the  $\gamma$ -position of caprolactone monomers in the thermo-responsive behavior of a series of self-assembled micellar systems utilizing MEEECL as the hydrophilic block (Figure 4). The resulting amphiphilic diblock copolymers were found to have an LCST in the range of 36–39 °C.<sup>15</sup>

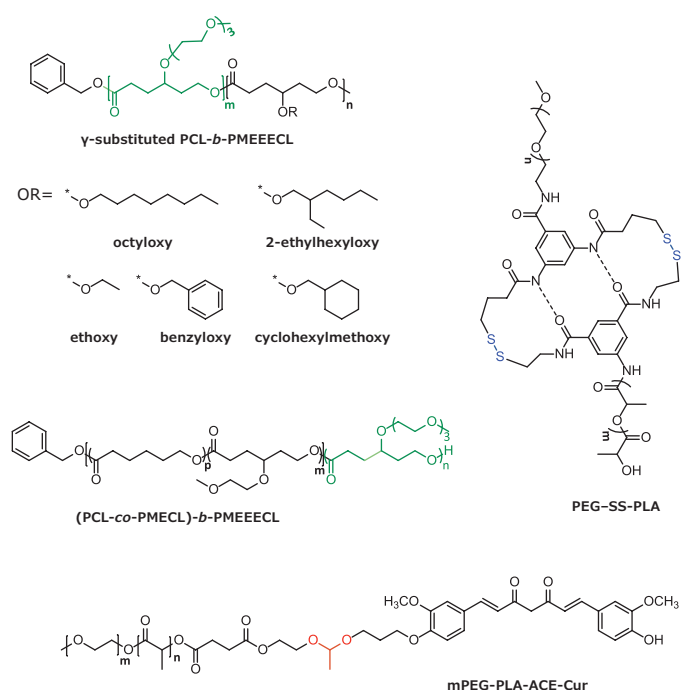


**Figure 4.** Single stimulus-responsive polyesters for drug delivery applications with responsive units highlighted (pH = red, temperature = green, and reduction = blue).

While polymer delivery systems that respond to a single stimulus have had a significant impact on the development of drug delivery technology, recent efforts have focused on systems that can respond to more than one stimulus. A dual pH- and redox-responsive system was reported by Ge and coworkers<sup>16</sup> in which copolymer prodrugs were encapsulated into PEG-*b*-PCL micelles. The copolymer prodrugs were prepared by the polymerization of pH-responsive 2-(piperidin-1-yl)ethyl methacrylate (PEMA) and reduction-responsive camptothecin (CPT, **Prod. No. C9911**). Due to the protonation of PPEMA in acidic pH, the zeta potential of the micelles increased from -2 mV to +12 mV, resulting in an increase of the size of the micelles from 32.7 to 48.6 nm. 80% of CPT was released by the cleavage of the disulfide bonds in response to increased GSH concentration. Thermo- and pH-responsive micelles designed by Chen and coworkers consist of a hydrophobic PCL segment and a thermo-responsive poly(*N*-isopropylacrylamide) (PNIPAM) hydrophilic segment, which was copolymerized with a pH-sensitive  $\beta$ -alanine-functionalized monomer (BA).<sup>17</sup> The micelles were co-loaded with DOX and a photosensitizer, meso-tetraphenylchlorin. The LCST of this polymer decreased from 37 °C at pH 7.4 to 25.8 °C at pH 6.0, resulting in the release of the encapsulated drug in acidic conditions. Consequently, 70% and 40% of DOX was released in acidic and neutral environments, respectively.

Zhao and coworkers designed a multi-responsive, comb-like copolymer by grafting a copolymer of PEG, PCL, and a reduction-responsive disulfide bond to a thermo-responsive PNIPAM backbone via a pH-responsive acetal linkage (Figure 5).<sup>10</sup> This dual-cleavable, multi-responsive, graft copolymer aggregate demonstrated high DOX release after stimuli application. Cumulative DOX release was studied in different conditions, including neutral and acidic pH, elevated temperature, and in the presence or absence of DTT. A maximum release of 77.1% was observed at 37 °C, pH 5.3, and in the presence of DTT, in contrast to only 36.1% at 25 °C, pH 7.4, and without DTT. Although stimuli-responsive carriers increase the chance of accumulation in the targeted site, active targeting can be used to direct the drug delivery system to specific sites in the body.

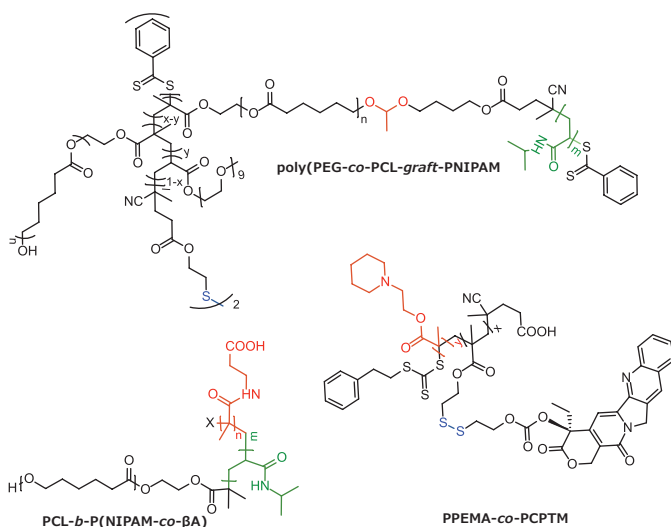


**Figure 5.** Multi stimuli-responsive polyesters for drug delivery applications with responsive units highlighted (pH = red, temperature = green, and reduction = blue).

### Active Targeted Polyester Drug Carriers

Compared to passive targeting, targeted drug delivery allows for the delivery of encapsulated drugs to the targeted site, reducing the risk of toxicity to normal cells and allowing for the accumulation of drug in sufficient concentrations to eliminate tumor cells. A comparison of passive and active targeting is shown in Figure 6. Targeting moieties are typically attached to the polymer through end-group variation or conjugation along the polymer backbone. A wide spectrum of targeting moieties can be used, including antibodies, proteins, peptides, carbohydrates, vitamins, and nucleic acids.<sup>3</sup>

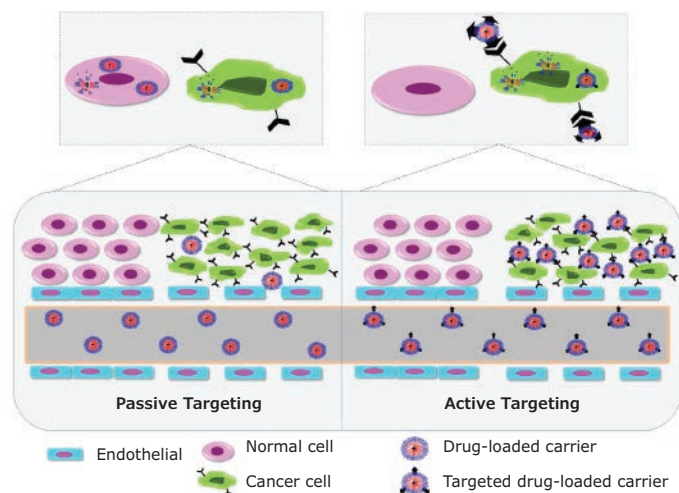


**Figure 6.** Graphical representation of passive versus active targeting.

A biodegradable polymeric matrix with disulfide linkages (PEG-SS-PCL) from Zhong et al. was functionalized with cyclic arginine-glycine-aspartic acid (cRGD) peptide to form a cRGD/PEG-SS-PCL nanomicelle, which exhibited high affinity for  $\alpha_v\beta_3$  integrins.  $\alpha_v\beta_3$  integrins are important biomarkers overexpressed on angiogenic tumor endothelial cells and malignant tumor cells, such as U87MG glioblastoma cells and B16 melanoma cells. These DOX-loaded, functionalized nanomicelles showed a half-maximal inhibitory concentration ( $IC_{50}$ ) of 6.36  $\mu\text{g}/\text{mL}$ , 2.9-fold lower than that of the non-functionalized micelle ( $IC_{50} = 18.35 \mu\text{g}/\text{mL}$ ). *In vivo* biodistribution was performed using U87MG tumor-bearing nude mice. Four hours post injection *ex vivo* DOX fluorescence imaging revealed that DOX delivered via cRGD/PEG-SS-PCL exhibited higher accumulation in the tumor (4.38% ID/g) in comparison to liver, heart, spleen, lung, and kidney tissue. In addition, this was also 2.2-fold higher than that of DOX delivered via PEG-SS-PCL (1.99% ID/g).<sup>18</sup>

Zhou and coworkers reported a dual-responsive polymer micelle generated from the self-assembly of a redox-responsive prodrug, a mPEG-SS-CPT and phenylboronic acid (PBA) functionalized enzyme-responsive copolymer, and PBA-PEG-4,4'-(diazene-1,2-diyl)benzoyl-PCL (PBA-PEG-Azo-PCL). PBA interacts with sialic acid, which is overexpressed in hepatoma carcinoma cells, enhancing *in vitro* cellular uptake in HepG2 cells with the PBA-functionalized carrier. Moreover, strong fluorescence remained at the tumor site six hours post-injection in nude mice bearing H22 tumors, 1.84-fold higher than with the non-targeted micelle.<sup>19</sup>



Finally, poly(poly(ethylene glycol) methacrylate)–poly(caprolactone)–poly(poly(ethylene glycol) methacrylate) (pPEGMA–PCL– pPEGMA) triblock copolymer was conjugated with DOX through an acid-labile hydrazone bond. This pH responsive system was then functionalized with folic acid and/or AS1411 aptamer, which specifically bind to folate and nucleolin receptors, respectively, that are overexpressed in cancer cells. Using fluorescence-activated cell sorting, the cellular uptake of this dual-targeted system in MCF-7 and PANC-1 cells was found to be 10- and 100-fold higher compared to single and non-targeted nanoparticles, respectively. Moreover, L929, a noncancerous cell line showed no DOX adverse effects.<sup>20</sup>

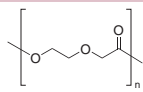
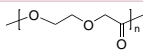
## Conclusion

Due to their versatility, biodegradable aliphatic polyesters have been shown to be excellent candidates in a wide range of anti-cancer drug delivery applications. Stimuli-responsiveness and targeted release of anti-cancer drugs with polyester drug carriers has improved the therapeutic efficacy while reducing adverse side effects to healthy cells. The structural and functional diversity of aliphatic polyesters provides new opportunities for creating novel materials with enhanced performance with dramatic impact on the development of next generation drug delivery systems. Progress in the development of aliphatic polyesters for anticancer drug delivery applications will continue to advance from the laboratory to clinical trials, improving both treatment options and patient outcomes in cancer therapy.

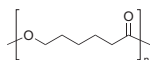
## Biodegradable Aliphatic Polyesters

For a complete list of available materials, visit [SigmaAldrich.com/biopoly](http://SigmaAldrich.com/biopoly).

### Poly(dioxanone)

Name	Structure	Viscosity (dL/g)	Prod. No.
Resomer® X 206 S, poly(dioxanone)		1.5-2.2	719846-1G 719846-5G
Dyed poly(dioxanone)		1.5	900320-5G
		2.0	900323-5G
		2.7	900324-5G

### Polycaprolactone

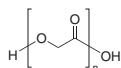


Name	Molecular Weight	Viscosity	Prod. No.
Polycaprolactone	$M_n \sim 10,000$ $M_w \sim 14,000$	400-1000 mPa.s	440752-5G 440752-250G 440752-500G
	-	1.5 dL/g	900297-5G
	$M_n$ 40,000-50,000 $M_w$ 48,000-90,000	-	704105-100G 704105-500G
	$M_n$ 80,000	-	440744-5G 440744-250G 440744-500G
	-	2.2 dL/g	900288-5G
	-	2.7 dL/g	900296-5G
	Dyed polycaprolactone	-	2.5 dL/g

## References

- Jones, M.-C.; Leroux, J.-C. *Eur. J. Pharm. Biopharm.* **1999**, *48*(2), 101.
- Harrison, K. In *Biomedical Polymers*; Jenkins, M., Ed.; Woodhead Publishing Series in Biomaterials; Woodhead Publishing, **2007**; pp 33–56.
- Washington, K. E.; Kularatne, R. N.; Karmegam, V.; Biewer, M. C.; Stefan, M. C. *Wiley Interdiscip. Rev. Nanomed. Nanobiotechnol.* **2016**, *9*(4), 1446.
- Coulember, O.; Degée, P.; Hedrick, J. L.; Dubois, P. *Prog. Polym. Sci.* **2006**, *31*(8), 723.
- Winzenburg, G.; Schmidt, C.; Fuchs, S.; Kissel, T. *Adv. Drug Deliv. Rev.* **2004**, *56*(10), 1453.
- Washington, K. E.; Kularatne, R. N.; Du, J.; Gillings, M. J.; Webb, J. C.; Doan, N. C.; Biewer, M. C.; Stefan, M. C. *J. Polym. Sci. Part A Polym. Chem.* **2016**, *54*(22), 3601.
- De Jong, W. H.; Borm, P. J. A. *Int. J. Nanomedicine* **2008**, *3*(2), 133.
- Uhrich, K. E.; Cannizzaro, S. M.; Langer, R. S.; Shakesheff, K. M. *Chem. Rev.* **1999**, *99*(11), 3181.
- Yu, D.; Zou, G.; Cui, X.; Mao, Z.; Estrela-Lopis, I.; Donath, E.; Gao, C. *J. Mater. Chem. B* **2015**, *3*(45), 8865.
- Liu, H.; Li, C.; Tang, D.; An, X.; Guo, Y.; Zhao, Y. *J. Mater. Chem. B* **2015**, *3*(19), 3959.
- Li, M.; Gao, M.; Fu, Y.; Chen, C.; Meng, X.; Fan, A.; Kong, D.; Wang, Z.; Zhao, Y. *Colloids Surf., B* **2016**, *140*, 11.
- Yang, Q.; Tan, L.; He, C.; Liu, B.; Xu, Y.; Zhu, Z.; Shao, Z.; Gong, B.; Shen, Y.-M. *Acta Biomater.* **2015**, *17*, 193.
- Rainbolt, E. A.; Washington, K. E.; Biewer, M. C.; Stefan, M. C. *J. Mater. Chem. B* **2013**, *1*(47), 6532.
- Cheng, Y.; Hao, J.; Lee, L. A.; Biewer, M. C.; Wang, Q.; Stefan, M. C. *Biomacromolecules* **2012**, *13*(7), 2163.
- Hao, J.; Cheng, Y.; Ranatunga, R. J. K. U.; Senevirathne, S.; Biewer, M. C.; Nielsen, S. O.; Wang, Q.; Stefan, M. C. *Macromolecules* **2013**, *46*(12), 4829.
- Huang, M.; Zhao, K.; Wang, L.; Lin, S.; Li, J.; Chen, J.; Zhao, C.; Ge, Z. *ACS Appl. Mater. Interfaces* **2016**, *8*(18), 11226.
- Chen, C.-Y.; Wang, Y.-C.; Hung, C.-C. *React. Funct. Polym.* **2016**, *98*, 56.
- Zhu, Y.; Zhang, J.; Meng, F.; Deng, C.; Cheng, R.; Feijen, J.; Zhong, Z. *J. Control. Release* **2016**, *233*, 29.
- Zhang, L.; Wang, Y.; Zhang, X.; Wei, X.; Xiong, X.; Zhou, S. *ACS Appl. Mater. Interfaces* **2017**, *9*(4), 3388.
- Lale, S. V.; R. G., A.; Aravind, A.; Kumar, D. S.; Koul, V. *Biomacromolecules* **2014**, *15*(5), 1737.

## Polyglycolide



Name	Viscosity at 25 °C (dL/g)	Degradation Time	Prod. No.
Polyglycolide	1.1-1.7	6-12 months	457620-1G 457620-5G 457620-10G

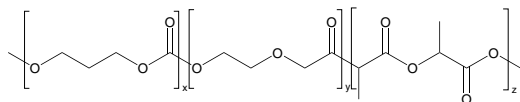
## Poly lactide



Name	Molecular Weight	Viscosity at 25 °C (dL/g)	Degradation Time	Prod. No.
Poly(D,L-lactide)	M <sub>w</sub> 15000	-	<6 months	805734-5G
Resomer® R 202 H, Poly(D,L-lactide)	M <sub>w</sub> 10,000-18,000	0.16-0.24	<6 months	719978-1G 719978-5G
Resomer® R 202 S, Poly(D,L-lactide)	M <sub>w</sub> 10,000-18,000	0.16-0.24	<6 months	719951-1G 719951-5G
Poly(D,L-lactide)	M <sub>w</sub> 75,000-120,000	0.55-0.75	12-16 months	531162-1G 531162-5G
Resomer® R 203 H, Poly(D,L-lactide)	M <sub>w</sub> 18,000-24,000	0.25-0.35	<6 months	719943-1G 719943-5G
Resomer® L 206 S, Poly(L-lactide), ester terminated	-	0.8-1.2	>3 years	719854-5G 719854-25G
Poly(L-lactide)	M <sub>n</sub> 50,000	-	>3 years	94829-1G-F 94829-5G-F
	-	1.5	-	900295-5G

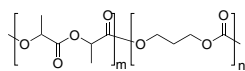
## Copolymers

### Poly(dioxanone)



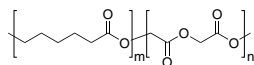
Name	Monomer Ratio	Viscosity (dL/g)	Prod. No.
Poly(trimethylene carbonate-co-p-dioxanone-co-L-lactide)	trimethylene carbonate:p-dioxanone:lactide 14:7:79	1.5	900325-5G
Poly(p-dioxanone-co-glycolide-co-lactide)	p-dioxanone:glycolide:lactide 90:5:5	2.0	900326-5G

### Poly(lactide-co-trimethylene carbonate)



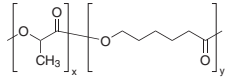
Name	Lactide:Trimethylene Carbonate	Viscosity (dL/g)	Prod. No.
Poly(L-lactide-co-trimethylene carbonate)	60:40	0.75	900311-5G
	10:90	0.75	900319-5G
	40:60	1.0	900317-5G
	20:80	1.5	900318-5G
Poly(D,L-lactide-co-trimethylene carbonate)	50:50	1.5	900327-5G

### Poly(caprolactone-co-glycolide)



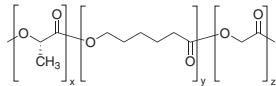
Name	Caprolactone:Glycolide	Viscosity (dL/g)	Prod. No.
Poly(caprolactone-co-glycolide)	90:10	0.75	900292-5G
	95:5	1.0	900291-5G
	45:55	1.5	900313-5G
	25:75	1.6	900314-5G

### Poly(lactide-co-caprolactone)



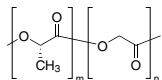
Name	Lactide:Caprolactone	Viscosity (dL/g)	Prod. No.
Poly(D,L-lactide-co-caprolactone)	40:60	0.7-0.9	457639-5G
	85:15	0.7-0.9	457647-5G
Poly(L-lactide-co-caprolactone)	35:65	1.5	900321-5G
	15:85	1.5	900312-5G

### Poly(caprolactone-co-glycolide-co-lactide)



Name	Lactide:Caprolactone:Glycolide	Prod. No.
Poly(L-lactide-co-caprolactone-co-glycolide)	70:20:10	568562-1G 568562-5G

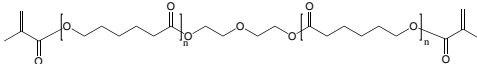
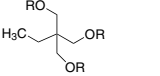
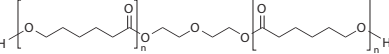
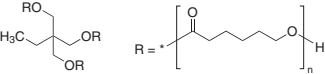
### Poly(lactide-co-glycolide)



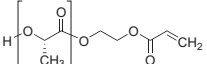
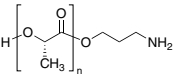
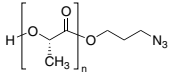
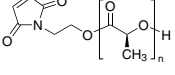
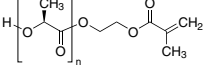
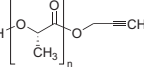
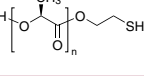
Name	Lactide:Glycolide	Molecular Weight	Viscosity At 25 °C (dL/g)	Degradation Time (months)	Prod. No.
Poly(L-lactide-co-glycolide)	5:95	-	1.1	<4	790214-1G 790214-5G
	20:80	-	1.6	-	900289-5G
Resomer® RG 502, Poly (D,L-lactide-co-glycolide)	50:50	7,000-17,000	0.16-0.24	<3	719889-1G 719889-5G
Resomer® RG 502 H, Poly (D,L-lactide-co-glycolide)	50:50	7,000-17,000	0.16-0.24	<3	719897-1G 719897-5G
Resomer® RG 503, Poly (D,L-lactide-co-glycolide)	50:50	24,000-38,000	0.32-0.44	<3	739952-1G 739952-5G
Resomer® RG 503 H, Poly (D,L-lactide-co-glycolide)	50:50	24,000-38,000	0.32-0.44	<3	719870-1G 719870-5G
Resomer® RG 504, Poly (D,L-lactide-co-glycolide)	50:50	38,000-54,000	0.45-0.60	<3	739944-1G 739944-5G
Resomer® RG 504 H, Poly (D,L-lactide-co-glycolide)	50:50	38,000-54,000	0.45-0.60	<3	719900-1G 719900-5G
Resomer® RG 505, Poly (D,L-lactide-co-glycolide)	50:50	54,000-69,000	0.61-0.74	<3	739960-1G 739960-5G
Poly(L-lactide-co-glycolide)	65:35	-	0.6	-	900316-5G
Resomer® RG 653 H, Poly (D,L-lactide-co-glycolide)	65:35	24,000-38,000	0.32-0.44	<5	719862-1G 719862-5G
Poly(D,L-lactide-co-glycolide)	65:35	40,000-75,000	-	-	P2066-1G P2066-5G
Resomer® RG 752 H, Poly (D,L-lactide-co-glycolide)	75:25	4,000-15,000	0.14-0.22	<6	719919-1G 719919-5G
Poly(D,L-lactide-co-glycolide)	75:25	66,000-107,000	-	-	P1941-1G P1941-5G
Resomer® RG 756 S, Poly (D,L-lactide-co-glycolide)	75:25	76,000-115,000	0.71-1.0	<6	719927-1G 719927-5G
Poly(D,L-lactide-co-glycolide)	85:15	50,000-75,000	0.55-0.75	<6	430471-1G 430471-5G
Resomer® RG 858 S, Poly (D,L-lactide-co-glycolide)	85:15	190,000-240,000	1.3-1.7	<9	739979-1G 739979-5G

## Functionalized Biodegradable Polymers

### Polycaprolactone

Name	Structure	Molecular Weight	Prod. No.
Polycaprolactone dimethacrylate		1,350	802115-2G
		4,000	802158-2G
Polycaprolactone trimethacrylate	 $R = \left[ \text{O} \left( \text{CH}_2 \right)_5 \text{C}(=\text{O}) \right]_n$	950	799556-2G
Polycaprolactone diol		~530	189405-250G
			189405-500G
		~2,000	189421-250G 189421-500G
Polycaprolactone triol		~300	200387-250G
			200387-500G
		~900	200409-250G 200409-500G

### Poly(lactide)

Name	Structure	Molecular Weight	Prod. No.
Poly(L-lactide), acrylate terminated		2,500	775991-1G
		5,500	775983-1G
Poly(L-lactide), amine terminated		2,500	776378-1G
			776378-5G
		4,000	776386-1G 776386-5G
Poly(L-lactide), azide terminated		5,000	774146-1G
Poly(L-lactide), N-2-hydroxyethyl maleimide terminated		2,000	746797-1G
		5,000	746797-5G 746517-1G 746517-5G
Poly(L-lactide), 2-hydroxyethyl methacrylate terminated		2,000	771473-1G
			771473-5G
		5,500	766577-1G 766577-5G
Poly(L-lactide), propargyl terminated		2,000	774162-1G
		5,000	774154-1G
Poly(L-lactide), thiol terminated		2,500	747386-1G
			747386-5G
		5,000	747394-1G 747394-5G

# Polymersomes for Drug Delivery



Joe Collins, Ayana Bhaskaran,  
Luke Andrew Connal\*

Department of Chemical Engineering,  
Melbourne School of Engineering  
The University of Melbourne, Parkville 3010  
Victoria, Australia

\*Email: luke.connal@unimelb.edu.au

## Introduction

The development of drugs that target specific locations within the human body remains one of the greatest challenges in biomedicine today. The majority of currently administered drugs have no means of targeting specific tissues or cells. Non-specific drug activity on healthy cells can lead to serious side-effects, drastically reducing a patient's quality of life. For example, chemotherapy typically leads to severe side effects such as hair loss, loss of the lining of the gut, ulcer formation, nausea, and more. Specific drug targeting has the potential to reduce or eliminate side effects and allow for a reduction in the dosage required, thus decreasing cost while increasing therapeutic efficiency and improving the quality of life. Although modern methods for drug delivery have improved selectivity, significant problems such as drug degradation, low bioavailability, and limited circulation times remain. An ideal drug delivery system should offer stability, targeting to a specific site within the body, and controlled release upon delivery to the target site.

Polymersomes, colloidal-sized hollow spheres comprised of an aqueous core surrounded by a polymeric bilayer membrane, are promising candidates for next generation drug delivery systems (Figure 1). Inspired by nature, polymersomes are synthetic analogs to liposomes found in all living cells. Formed by the self-assembly of amphiphilic molecules, polymersomes are capable of transporting hydrophilic molecules (loaded within the aqueous core of the polymersomes), hydrophobic molecules (loaded within the membrane bilayer), or a combination of both—allowing a greater therapeutic action than a single drug alone (Figure 1).<sup>1</sup> Polymersomes feature enhanced toughness,<sup>2</sup> reduced membrane permeability,<sup>2</sup> and possess little to no immunogenicity (if designed correctly).<sup>3</sup> These block copolymer vesicles can achieve targeted drug delivery through surface functionalization with ligands for specific cell receptors (e.g., proteins, carbohydrates, or small molecules). The controlled drug release from within polymersome capsules can be achieved through the incorporation of stimuli-responsive chemistry. Due to these benefits, polymersomes have been extensively explored in various biomedical applications such as drug delivery,<sup>3,4</sup> gene and protein delivery,<sup>5</sup> imaging,<sup>6</sup> and diagnostics.<sup>7</sup> This article will focus specifically on polymersomes for drug delivery.

Polymersome synthesis will be discussed followed by a review of surface functionalization to achieve polymersome targeting and the incorporation of dynamic or stimuli-responsive chemistry for controlled drug release.

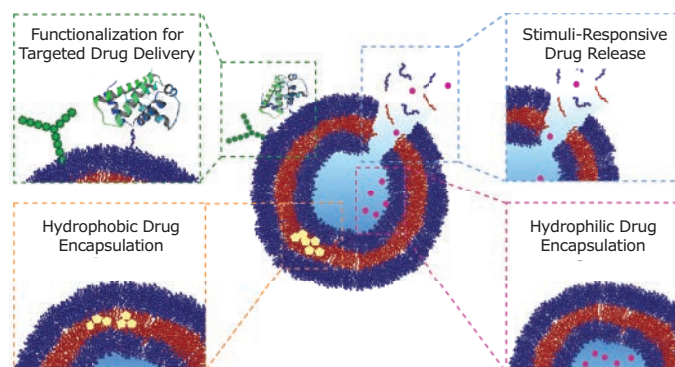


**Figure 1.** Schematic highlighting the advantages of polymersomes for drug delivery. Surface functionalization of polymersomes with carbohydrates, proteins, or small molecules allows for polymersome targeting to specific locations within the body (green box). Stimuli-responsive drug release allows for controlled drug delivery (blue box) of hydrophilic drug molecules, loaded within the polymersomes core (pink box) and hydrophobic drug molecules, loaded within the polymersome membrane bilayer (orange box).

## Fabrication Process: Design, Synthesis and Drug Encapsulation

The development of controlled radical polymerization (CRP) techniques, such as nitroxide-mediated polymerization (NMP), reversible addition-fragmentation chain transfer polymerisation (RAFT), and atom-transfer radical polymerisation (ATRP), has allowed for the synthesis of well-defined, amphiphilic polymers (for example, PS-*b*-PAA, Figure 2A). Through CRP, polymers with precise molecular weights, low dispersity ( $\mathcal{D}$ ), and specific architectures can be synthesized. Examples include block copolymers (BCPs), triblock copolymers, and graft polymers. A wide range of amphiphilic polymers have been successfully synthesized through CRP and shown to self-assemble into interesting structures such as spheres/micelles, cylinders, and polymersomes.<sup>8</sup>

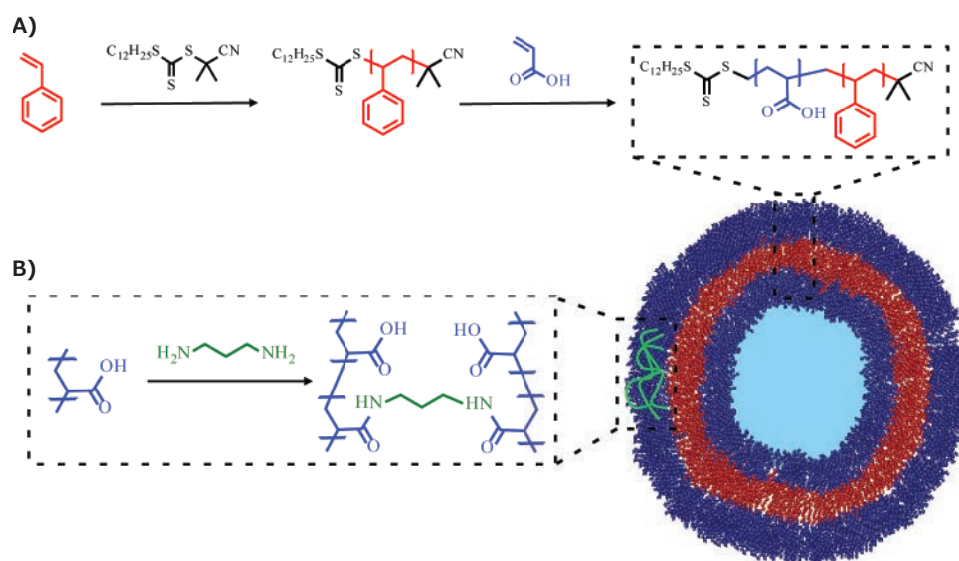


**Figure 2.** Representative synthesis of BCP via RAFT polymerization and BCP self-assembly into polymersomes, as well as polymersome stabilization through crosslinking. **A)** A hydrophobic block of polystyrene (PS) is produced by RAFT polymerization. From this is grown a hydrophilic polymer block of poly(acrylic acid) (PAA). Self-assembly of the PS-*b*-PAA BCP yields polymersome capsules. **B)** Crosslinking can be utilized to increase the stability of polymersomes represented here by amide formation between poly(acrylic acid) chains.

The self-assembly of BCPs in solution is governed by the packing parameter ( $p$ ). The packing parameter can be used to indicate what structure will be formed upon self-assembly by taking into account the volume of the hydrophobic chain ( $v$ ), the interfacial area per molecule ( $a$ ), and the length of the hydrophobic chain ( $l$ ) (Eq. 1). Different structures fall between different  $p$  values; if  $p < 1/3$  spherical structures will form, between  $1/3 < p < 1/2$  cylinders will form, and  $1/2 < p < 1$  polymersomes will form.

$$p = \frac{v}{al}$$

**Equation 1.** Packing parameter of amphiphilic BCPs.

The synthesis of polymersomes usually involves the slow addition of a select solvent to a dissolved solution containing the amphiphile. As the solvent properties change, amphiphiles self-assemble to minimize unwanted solvent-polymer interactions. A number of techniques have been developed for the preparation and characterization of polymersomes.<sup>8</sup>

Since only non-covalent forces govern polymersome assembly and stability, these supramolecular structures are inherently unstable, which is amplified upon introduction to areas of massive dilution, such as the blood stream. The stability of polymersomes can be increased by covalently crosslinking the hydrophobic core, hydrophilic shell, or core-shell interface. Crosslinking has been reported using diverse chemistries including amide, disulfide, UV-irradiation, and carbodiimide coupling. These and other means of polymersome crosslinking have been reviewed previously.<sup>3,4</sup>

Polymersomes have attracted great interest for drug delivery applications due to high drug loading capability and the ability to

carry both hydrophilic and hydrophobic molecules. Hydrophobic molecules integrate into the non-aqueous membrane bilayer and hydrophilic molecules are captured inside the aqueous core. A wide range of hydrophobic and hydrophilic molecules have been successfully loaded into polymersomes.<sup>3,4</sup> Specific examples include membrane proteins, hydrophobic drugs (e.g., Paclitaxel), hydrophobic molecules (e.g., camptothecin, **Prod. No. C9911**), and hydrophilic drugs (e.g., Doxorubicin hydrochloride [DOX HCl], **Prod. No. D1515**). The ability to load both hydrophobic and hydrophilic molecules simultaneously into polymersomes often results in far greater therapeutic effect than a single drug alone. A report by Thambi et al. describes the synthesis of a redox-responsive polymersome composed of the triblock copolymer PEG-*b*-PLys-SS-PCL which was successfully loaded with DOX HCl (in the aqueous core) and camptothecin (in the membrane bilayer). Higher cytotoxicity was reported when the dual-drug loaded polymersome was utilized in comparison to a single administration of either drug alone.<sup>1</sup>

In general, drug release from polymersomes occurs through passive diffusion, driven by concentration gradients. The rate of diffusion can be tuned through modification of the bilayer membrane thickness, covalent crosslinking, and control over amphiphile composition. To overcome problems associated with non-specific drug release, many stimuli-responsive polymersomes have been developed to achieve controlled drug delivery at target locations.

### Functionalization for Targeted Drug Delivery

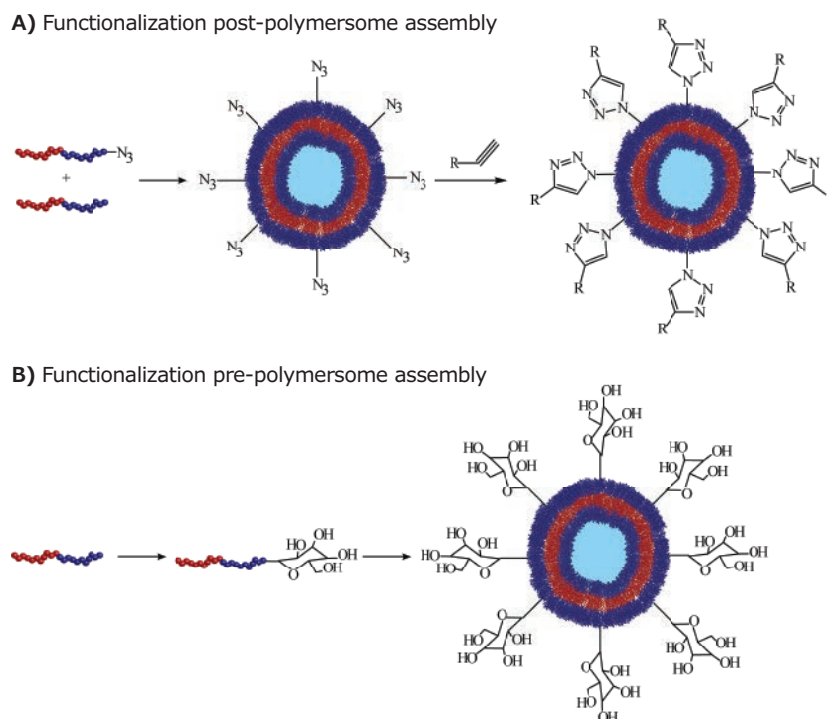
Polymersomes for targeted drug delivery feature surfaces functionalized with specific targeting groups and/or ligands. A range of molecules have been explored as targeting ligands (Table 1).

**Table 1.** Examples of ligands conjugated onto polymersome surfaces to achieve targeted drug delivery. The ligand receptor and corresponding site of action are noted.

Ligands	Receptor	Target/Pathology	References
<b>Small Molecules</b>			
Vitamin B7	Biotin Receptor	Cancer	9
Selegiline	Amyloid-beta peptide	Neurodegenerative diseases	10
Selectin	Activated endothelium	Inflammation	11
<b>Carbohydrates</b>			
Glucose/Lactose	Protein Receptor	Bioadhesion	12
Hyaluronan	CD44	Cancer	13
<b>Antibodies</b>			
OX26	Transferrin Receptor (TfR)	CNS	14
Epidermal Growth Factor	EGF Receptor	Cancer	15
Anti A $\beta$ 1-42 MAb	A $\beta$ 1-42 Peptide	Alzheimer's disease	16
<b>Peptides and Proteins</b>			
Tet1	Neuronal trisialoganglioside (GT1b) clostridial toxin receptor	Sensorineural Hearing Loss	17
Lactoferrin (Lf)	Lf Receptor	Brain	18
Insulin	Insulin Receptor	CNS	19

The conjugation of targeting molecules onto the surface of polymersomes can be achieved in two ways. In the first method, the targeting ligand is conjugated to active groups presented on the polymersome surface after polymersome formation (Figure 3A). Alternatively, the targeting ligand is conjugated onto the amphiphilic polymer prior to polymersome formation. The functionalized polymer is then allowed to assemble into

the final polymersome structure with the targeting ligand on its surface (Figure 3B). Both approaches are feasible for small molecules and peptides; however, larger molecules such as polysaccharides and proteins, must be incorporated post-polymersome formation, as they can act to disrupt the self-assembly of copolymer molecules into polymersomes.

**Figure 3.** Strategies for the incorporation of targeting groups onto a polymersome surface. **A)** Targeting groups can be added to reactive groups presented on the polymersome surface post-polymersome formation. This process is exemplified here through the conjugation of an alkyne-functionalized targeting group onto azide groups presented on a polymersome surface. **B)** Alternatively, the targeting group can be conjugated onto the amphiphilic polymer pre-polymersome formation. The functional polymer is then self-assembled into the final polymersome structure which displays the targeting groups on its surface. This process is exemplified here through the conjugation of a sugar molecule onto a block copolymer, which is then self-assembled into a polymersome displaying the sugar groups on its surface.

Several attempts have been made to conjugate ligands on preformed polymersomes using click chemistry.<sup>20,21</sup> Due to their high efficiency and orthogonality, click reactions are an effective method to achieve a high degree of surface functionalization. For example, van Hest and coworkers synthesized polymersomes composed of an azide-functionalized amphiphilic polystyrene-*block*-poly(acrylic acid) (PS-*b*-PAA-N<sub>3</sub>) copolymer.<sup>20</sup> The copper-catalyzed azide-alkyne (CuAAC) reaction was then used to bind an alkyl-bearing fluorescent dansyl probe and/or biotin onto the polymersome surface, allowing for effective surface functionalization.<sup>20</sup> Martin et al. also used the CuAAC reaction to conjugate alkyne-functional dendritic and non-dendritic mannose derivatives onto polymersomes comprised of azide-functional poly(butadiene-*block*-ethylene oxide-N<sub>3</sub>) BCP.<sup>21</sup> The dendritic derivatives displayed a two-fold higher binding affinity towards concanavalin A than the non-dendritic derivatives.<sup>21</sup>

As mentioned previously, targeting ligands can be grafted onto the end of the amphiphilic BCP prior to polymersome formation. As the ratio of functional to non-functional BCP can be controlled, the surface density of the targeting ligand in the final polymersome assembly can also be easily tuned. This is an advantage over functionalization post-polymersome formation, in which control over the degree of surface functionalization is much more limited. Utilizing the pre-polymersome functionalization strategy, Kim et al. successfully managed to target *E. coli* bacteria with a mannose-functionalized tetra(*p*-phenylene)-*block*-PEG copolymer. The self-assembled polymersomes were reported to display an 800-fold increase in the binding affinity towards *E. coli* pili compared to non-functionalized polymersomes.<sup>22</sup>

Significant efforts have been made to improve the potency of chemotherapy by targeting the active drug to the tumor site. Polymersomes have been successfully used to target different sites within the body, such as the central nervous system (CNS), brain, cochlea, and macrophages (Figure 4).<sup>8</sup> Certain cell surface receptors are over expressed in human cancer cell lines including breast, prostate, colorectal, and lung cancer cells.<sup>3,8</sup> This can be exploited for polymersome targeting through the conjugation of specific binding ligands onto the polymersome surface. Alternatively, many cancers overexpress certain enzymes. Careful design of block copolymers, in which the polymer blocks are linked via enzyme cleavable groups, enables specific drug release once the polymersome has entered the target cell. Jung et al. developed biodegradable polymersomes from methoxy poly(ethylene glycol) and poly(D,L-Lactide) diblock copolymers, with a connecting peptide sequence Gly-Phe-Leu-Gly-Phe (GFLGF) that is cleavable by lysosomal enzymes present in tumor cells.<sup>14</sup> Antibody-mediated endocytosis followed by the cleavage of the peptide sequence in the resulting polymer (mPEG-GFLGF-PDLLA), leads to dissolution of the polymersome and concurrent drug release.

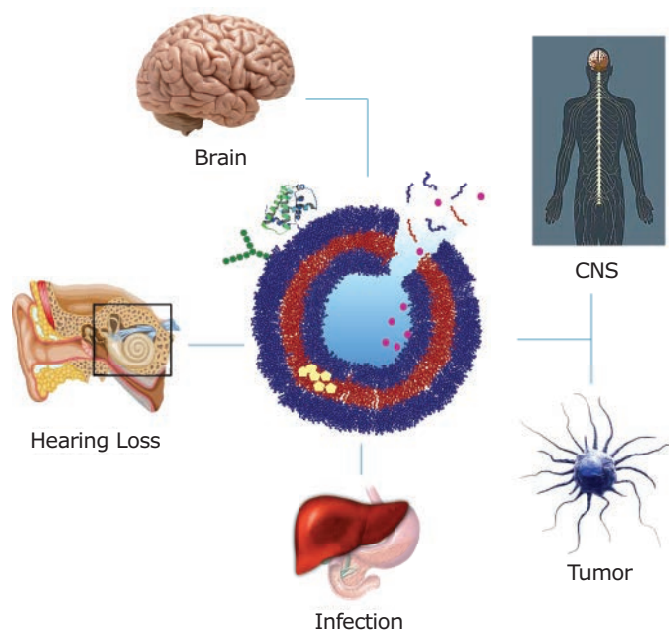


**Figure 4.** Functionalized polymersomes are used for diagnostic and therapeutic applications. Targeted drug delivery to various organs have major research focus on neurodegenerative diseases, cancer treatment, sensorineural hearing loss, infection and inflammation detected in the CNS, brain, tumor cells, cochlea, and macrophages, respectively.

Once polymersomes are targeted to specific locations, the encapsulated drug must be released to attain a therapeutic effect. Controlled drug release can be achieved through the incorporation of stimuli-responsive chemistry into the polymersome structure.

### Responsive Drug Release

By incorporating a variety of dynamic or responsive chemistries into the polymer building blocks, polymersomes can be designed to release their payload upon the application of a diverse range of stimuli. The ability to trigger drug release at target locations allows for superior drug activity and the minimization of unwanted side effects. In general, stimuli-responsive drug release from polymersomes is achieved through three mechanisms: cleavage of a stimuli-responsive group linking the polymer blocks (Figure 5, red), degradation of the intermolecular bonds between monomer units in a polymer block (Figure 5, blue), or through an electrostatic change in one of the polymer blocks resulting in a shift from a hydrophobic to hydrophilic state (Figure 5, green). All three mechanisms result in the dissolution or degradation of the polymersome and release of the encapsulated cargo.

Many examples of stimuli have been reported to achieve drug release from polymersomes such as pH, redox, reaction with reactive-oxygen species or glucose, or through the application of external stimuli such as a magnetic field, ultrasound, or light. Several recent comprehensive reviews have described the



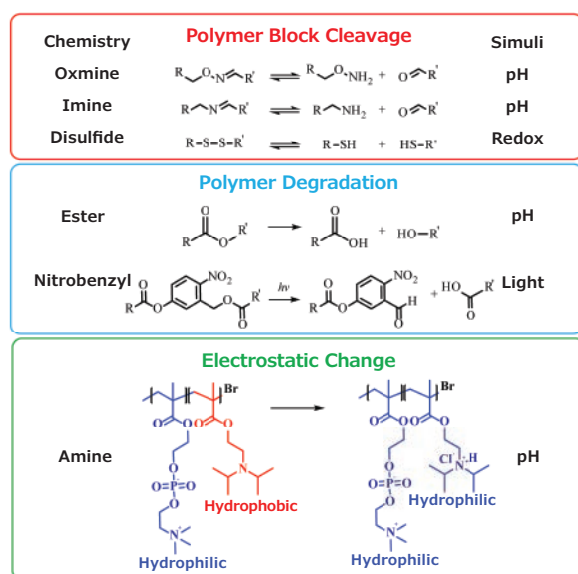
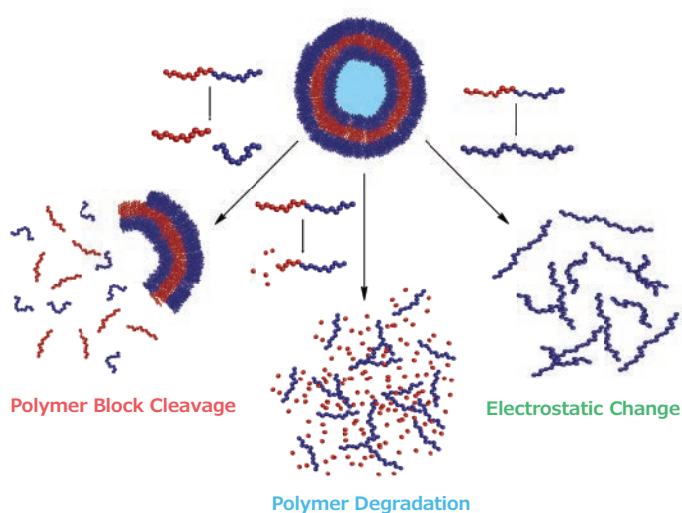


**Figure 5.** Degradation/dissolution of polymersomes by polymer block cleavage (red), polymer degradation (blue), or through an electrostatic change (green).

synthesis and applications of stimuli-responsive polymersomes.<sup>3,4</sup> The three most researched stimuli are pH, redox potential, and light. Two rely on naturally occurring physiological gradients (pH and redox potential), while the other relies on the application of an external stimulus (light).

The development of pH-responsive polymersomes has received significant attention due to naturally occurring pH gradients in the body. Physiological pH is balanced around pH 7.4, with lower pH environments occurring in inflammatory and tumor tissue (pH 6.5–7.2) and inside lysosomes and endosomes (pH 4.5–5.5). This provides a facile means to achieve polymersome degradation and drug release through the incorporation of pH-sensitive or ionizable bonds in the amphiphilic polymer.

Block copolymers with a hydrophobic block comprised of a hydrolytically degradable polyester, such as poly(lactic acid) (PLA) or poly( $\epsilon$ -caprolactone) (PCL), were some of the earliest pH-sensitive polymersomes developed.<sup>23</sup> Polymersome dissolution (and drug release) is achieved through hydrolysis of

the ester bonds linking the polymer blocks. PEG-*b*-PCL and PEG-*b*-PLA polymersomes, loaded with DOX or Paclitaxel, were shown to localize in tumor tissue in mice and release the encapsulated payload upon entering the acidic tumor environment, arresting tumor growth and yielding tumor shrinkage.<sup>24</sup>

An alternate method of pH-stimulated drug delivery from polymersome vesicles, involves linking the polymer blocks through a pH-sensitive bond, such as an imine, hydrazone, or acetal.<sup>4</sup> Upon exposure to acidic conditions, the link between the hydrophilic and hydrophobic block degrades, leading to the breakdown of the polymersome and release of the encapsulated cargo.

pH-triggered polymersome degradation can also be obtained through the incorporation of an ionizable group into one of the polymer blocks. Examples include the synthesis of a zwitterionic poly(2-(methacryloyloxy)ethylphosphorylcholine)-*b*-poly(2-(diisopropylamino)ethyl methacrylate) (PMPC-*b*-PDPA) block copolymer prepared by Armes and co-workers.<sup>25</sup> The PMPC-*b*-PDPA polymersome was designed to be stable at physiological pH, but degradable under acidic conditions. Degradation was achieved through the protonation of the tertiary amine groups of PDPA, which prior to protonation is hydrophobic but becomes hydrophilic upon protonation, resulting in polymersome dissolution. Due to the acidic  $pK_a$  of the amine (6.4) in PDPA, the polymersomes are stable in the bloodstream at physiological pH (7.4) but degradable under the acidic conditions found in lysosomes and endosomes.

Redox active polymers are a versatile platform for targeted drug delivery, as redox potentials vary greatly between normal and tumor tissue, the intracellular and extracellular environment, and even between different cell organelles. Glutathione (GSH), an important cellular reducing agent, is often used to trigger the reduction of sensitive linkages for polymersome disassembly. GSH concentrations are typically very low in plasma and normal tissue (2–20  $\mu$ M) but significantly higher in the cytosol, nuclei, and tumor tissue (2–20 mM), producing a high intracellular redox gradient. Disulfide (-S-S-) bonds are susceptible to reduction by GSH, to produce two thiol (-SH) groups. This has been exploited for target drug delivery by incorporating disulfide bonds into the polymer backbone of polymersomes, such as in the synthesis of the triblock copolymer PEG-MA-*b*-PCL-S-S-PCL-*b*-PEG-MA<sup>26</sup> or as a chemical crosslinker as in the case of a PEG-*b*-PLys-*b*-PCL polymersome.<sup>27</sup> GSH reduction and subsequent disulfide cleavage leads to polymersome disassembly and the release of the encapsulated payload.

Light is an attractive means of triggering drug release, as it allows for a high degree of temporal and spatial control, and uses a non-invasive method. Using light to trigger drug release from polymersomes is usually achieved either through a structural change in the polymersome or through polymer degradation through light irradiation. A variety of light-sensitive groups have been introduced into polymersomes such as spiropyran, 2-nitrophenylalanine, and *o*-nitrobenzyl; these have been reviewed previously by Hu et al.<sup>4</sup>

## Conclusion

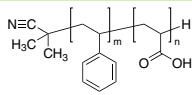
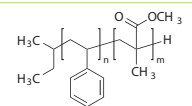
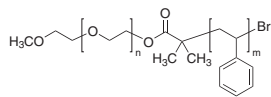
The unique characteristics of polymersomes make them highly promising materials for drug delivery applications. We have summarized the design and fabrication considerations for polymersomes, highlighting drug encapsulation procedures. The ability to functionalize the polymersome surface for active targeting and for controlled drug release demonstrates the power of these versatile nanomaterials.

## References

- Thambi, T.; Deepagan, V. G.; Ko, H.; Lee, D. S.; Park, J. H. *J. Mater. Chem.* **2012**, *22*, 22028.
- Discher, B. M.; Won, Y. Y.; Ege, D. S.; Lee, J. C. M.; Bates, F. S.; Discher, D. E.; Hammer, D. A. *Science*. **1999**, *284*, 1143.
- Anajafi, T.; Mallik, S. *Ther. Deliv.* **2015**, *6*, 521.
- Hu, X.; Zhang, Y.; Xie, Z.; Jing, X.; Bellotti, A.; Gu, Z. *Biomacromolecules* **2017**, *18*, 649.
- Onaca, O.; Enea, R.; Hughes, D. W.; Meier, W. *Macromol. Biosci.* **2009**, *9*, 129.
- Tanner, P.; Baumann, P.; Enea, R.; Onaca, O.; Palivan, C.; Meier, W. *Acc. Chem. Res.* **2011**, *44*, 1039.
- Brinkhuis, R. P.; Rutjes, F. P. J. T.; van Hest, J. C. M. *Polym. Chem.* **2011**, *2*, 1449.
- Balasubramanian, V.; Herranz-Blanco, B.; Almeida, P. V.; Hirvonen, J.; Santos, H. A. *Prog. Polym. Sci.* **2016**, *60*, 51.
- Russell-Jones, G.; McTavish, K.; McEwan, J.; Rice, J.; Nowotnik, D. J. *Inorg. Biochem.* **2004**, *98*, 1625.
- Re, F.; Airoldi, C.; Zona, C.; Masserini, M.; Ferla, B. L.; Quattrocchi, N.; Nicotra, F. *Curr. Med. Chem.* **2010**, *17*, 2990.
- Ehrhardt, C.; Kneuer, C.; Bakowsky, U. *Adv. Drug Deliv. Rev.* **2004**, *56*, 527.
- Dwek, R. A. *Chem. Rev.* **1996**, *96*, 683.
- Turley, E. A.; Noble, P. W.; Bourguignon, L. Y. W. *J. Biol. Chem.* **2002**, *277*, 4589.
- Lee, J. S.; Groothuis, T.; Cusan, C.; Mink, D.; Feijen, J. *Biomaterials.* **2011**, *32*, 9144.
- Mendelsohn, J. *Endocr. Relat. Cancer.* **2001**, *8*, 3.
- Trauth, B. C.; Klas, C.; Peters, A. M.; Matzku, S.; Moeller, P.; Falk, W.; Debatin, K. M.; Krammer, P. H. *Science.* **1989**, *245*, 301.
- Liu, J. K.; Teng, Q.; Garrity-Moses, M.; Federici, T.; Tanase, D.; Imperiale, M. J.; Boulis, N. M. *Neurobiol. Dis.* **2005**, *19*, 407.
- Ji, B.; Maeda, J.; Higuchi, M.; Inoue, K.; Akita, H.; Harashima, H.; Suhara, T. *Life Sci.* **2006**, *78*, 851.
- Coloma, M. J.; Lee, H. J.; Kurihara, A.; Landaw, E. M.; Boado, R. J.; Morrison, S. L.; Pardridge, W. M. *Pharm. Res.* **2000**, *17*, 266.
- Opsteen, J. A.; Brinkhuis, R. P.; Teeuwen, R. L. M.; Löwik, D. W. P. M.; van Hest, J. C. M. *Chem. Commun.* **2007**, *7345*, 3136.
- Martin, A. L.; Li, B.; Gillies, E. R. *J. Am. Chem. Soc.* **2009**, *131*, 734.
- Kim, B.; Yang, W.; Ryu, J.; Yoo, Y.; Lee, M. *Chem. Commun.* **2005**, *15*, 2035.
- Meng, F.; Hiemstra, C.; Engbers, G. H. M.; Feijen, J. *Macromolecules.* **2003**, *36*, 3004.
- Ahmed, F.; Pakunlu, R. I.; Srinivas, G.; Brannan, A.; Bates, F.; Klein, M. L.; Minko, T.; Discher, D. E. *Mol. Pharm.* **2006**, *3*, 340.
- Du, J.; Tang, Y.; Lewis, A. L.; Armes, S. P. *J. Am. Chem. Soc.* **2005**, *127*, 17982.
- Kumar, A.; Lale, S. V.; Mahajan, S.; Choudhary, V.; Koul, V. *ACS Appl. Mater. Interfaces.* **2015**, *7*, 9211.
- Thambi, T.; Deepagan, V. G.; Ko, H.; Suh, Y. D.; Yi, G.-R.; Lee, J. Y.; Lee, D. S.; Park, J. H. *Polym. Chem.* **2014**, *5*, 4627.

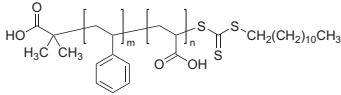
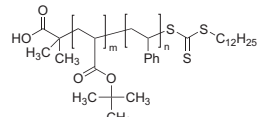
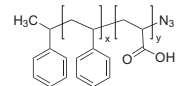
## Amphiphilic Block Copolymers

For a complete list of available materials, visit [SigmaAldrich.com/blockcopoly](http://SigmaAldrich.com/blockcopoly).

Name	Structure	Molecular Weight	Prod. No.
Poly(styrene)- <i>block</i> -poly(acrylic acid)		M <sub>n</sub> 27,000-31,000 (polystyrene) M <sub>n</sub> 4,000-6,000 (poly(acrylic acid))	<b>746991-1G</b>
Poly(styrene)- <i>block</i> -methyl methacrylate)		M <sub>n</sub> 27,000-31,000 (polystyrene) M <sub>n</sub> 1,000-2,000 (poly(acrylic acid))	<b>747009-500MG</b>
		M <sub>n</sub> 27,000-33,000 (polystyrene) M <sub>n</sub> 7,000-9,000 (poly(acrylic acid))	<b>746983-500MG</b>
		average M <sub>n</sub> 15,000 (polystyrene) average M <sub>n</sub> 15,000 (PMMA)	<b>749184-1G</b>
		average M <sub>n</sub> 22,000 (polystyrene) average M <sub>n</sub> 10,000 (PMMA)	<b>739553-1G</b> <b>739553-5G</b>
		average M <sub>n</sub> 57,000 (polystyrene) average M <sub>n</sub> 25,000 (PMMA)	<b>749206-1G</b>
average M <sub>n</sub> 52,000 (polystyrene) average M <sub>n</sub> 52,000 (PMMA)	<b>749192-1G</b>		
Poly(styrene)- <i>block</i> -poly(ethylene glycol)		M <sub>n</sub> 21,000-30,000 (polystyrene) M <sub>n</sub> 700-1,100 (PEG)	<b>686476-500MG</b>

## Functionalized Amphiphilic Block Copolymers

For a complete list of available materials, visit [SigmaAldrich.com/blockcopoly](http://SigmaAldrich.com/blockcopoly).

Name	Structure	Molecular Weight	Prod. No.
Poly(styrene)- <i>block</i> -poly(acrylic acid), DDMAT terminated		M <sub>n</sub> 2,700-3,300 (polystyrene) M <sub>n</sub> 4,000-6,000 (poly(acrylic acid))	<b>776351-500MG</b>
Poly(styrene)- <i>block</i> -poly( <i>tert</i> -butyl acrylate), DDMAT terminated, acid terminated		M <sub>n</sub> ~6,000 (polystyrene) M <sub>n</sub> ~6,000 (poly( <i>tert</i> -butyl acrylate))	<b>776432-1G</b>
Poly(styrene)- <i>block</i> -poly(acrylic acid), azide terminated		M <sub>n</sub> 5,500-6,000 (polystyrene) M <sub>n</sub> 2,600-2,950 (poly(acrylic acid))	<b>757594-250MG</b>
		M <sub>n</sub> 6,500-7,000 (polystyrene) M <sub>n</sub> 1,600-1,950 (poly(acrylic acid))	<b>735892-250MG</b>

## Biodegradable Amphiphilic Block Copolymers

For a complete list of available materials, visit [SigmaAldrich.com/blockcopoly](http://SigmaAldrich.com/blockcopoly).

### Poly(ethylene glycol)-*block*-poly(lactide)

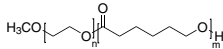
Name	Structure	Molecular Weight	Prod. No.
Poly(ethylene glycol)- <i>block</i> -poly(lactide) methyl ether		PEG average $M_n$ 350 PLA average $M_n$ 1,000	659665-1G
		PEG average $M_n$ 750 PLA average $M_n$ 1,000	659657-1G
Poly(ethylene glycol) methyl ether- <i>block</i> -poly(D,L lactide)		PEG average $M_n$ 2,000 PDLLA average $M_n$ 2,000	764779-1G
Poly(ethylene glycol) methyl ether- <i>block</i> -poly(D,L lactide)- <i>block</i> -decane		PEG average $M_n$ 2,000 PDLLA average $M_n$ 2,000	764736-1G
Poly(ethylene oxide)- <i>block</i> -poly(lactide), 4-arm		PEO $M_n$ ~2,500 PLA average $M_n$ ~3,500	570354-250MG 570354-1G
Poly(L-lactide)- <i>block</i> -poly(ethylene glycol) methyl ether		PEG average $M_n$ ~5,000 PLLA average $M_n$ ~5,000	570281-250MG 570281-1G
Methoxy poly(ethylene glycol)- <i>b</i> -poly(L-lactide)		PEG average $M_n$ ~2,000 PLLA average $M_n$ ~2,000	900703-500MG
		PEG average $M_n$ ~2,000 PLLA average $M_n$ ~5,000	900655-500MG
		PEG average $M_n$ ~5,000 PLLA average $M_n$ ~10,000	900656-500MG
Methoxy poly(ethylene glycol)- <i>b</i> -poly(D,L-lactide)		PEG average $M_n$ ~2,000 PDLLA average $M_n$ ~5,000	900657-500MG
		PEG average $M_n$ ~5,000 PDLLA average $M_n$ ~5,000	900658-500MG
		PEG average $M_n$ ~5,000 PDLLA average $M_n$ ~10,000	900659-500MG
		PEG average $M_n$ ~4,000 PDLLA average $M_n$ ~2,200	900661-500MG
		PEG average $M_n$ ~10,000 PDLLA average $M_n$ ~10,000	900663-500MG
		PEG average $M_n$ ~15,000 PDLLA average $M_n$ ~15,000	900681-500MG

### Poly(ethylene glycol)-*block*-poly(lactide-co-glycolide)

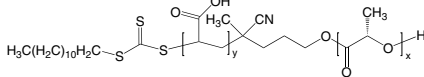
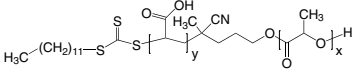
Name	Structure	Molecular Weight	Prod. No.
Poly(ethylene glycol) methyl ether- <i>block</i> -poly(L-lactide-co-glycolide)		PEG average $M_n$ 5,000 PLGA average $M_n$ 25,000	799041-1G
Poly(ethylene glycol) methyl ether- <i>block</i> -poly(lactide-co-glycolide)		PEG average $M_n$ 5,000 PLGA $M_n$ 7,000	765139-1G
		PEG average $M_n$ 5,000 PLGA $M_n$ 55,000	764752-1G
		PEG average $M_n$ 2,000 PLGA average $M_n$ 11,500	764760-1G
		PEG $M_n$ 2,000 PLGA $M_n$ 4,500	764825-1G
Poly(D,L-lactide-co-glycolide) (50:50)- <i>b</i> -poly(ethylene glycol)		PEG average $M_n$ ~2,000 PDLLA-co-PGA average $M_n$ ~10,000	900664-500MG

### Poly(ethylene glycol)-*block*-poly(caprolactone)

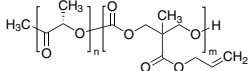
Name	Structure	Molecular Weight	Prod. No.
Poly(ethylene glycol)- <i>block</i> -poly( $\epsilon$ -caprolactone) methyl ether		PEG average $M_n$ ~5,000 PCL average $M_n$ ~5,000	570303-250MG 570303-1G
		PEG average $M_n$ ~5,000 PCL average $M_n$ ~13,000	570311-250MG 570311-1G
		PEG average $M_n$ ~5,000 PCL average $M_n$ ~32,000	570338-250MG 570338-1G

Name	Structure	Molecular Weight	Prod. No.
Methoxy poly(ethylene glycol)- <i>block</i> -poly( $\epsilon$ -caprolactone)		PEG average $M_n \sim 2,000$	900649-500MG
		PCL average $M_n \sim 2,000$	
		PEG average $M_n \sim 2,000$	900648-500MG
		PCL average $M_n \sim 5,000$	
PEG average $M_n \sim 5,000$	PCL average $M_n \sim 10,000$	900672-500MG	
		PEG average $M_n \sim 5,000$	PCL average $M_n \sim 2,000$

### Poly(lactide)-*block*-poly(acrylic acid)

Name	Structure	Molecular Weight	Prod. No.
Poly(L-lactide)- <i>block</i> -acrylic acid)		PLLA average $M_n 10,000$	799246-1G
		PAA average $M_n 8,000$	
Poly(D,L-lactide)- <i>block</i> -acrylic acid)		PLLA $M_n 4,500$	805718-1G
		PAA $M_n 18,000$	
PDLLA $M_n 5,000$	PAA $M_n 18,000$	798126-1G	
		PDLLA $M_n 18,000$	PAA $M_n 11,000$
PDLLA average $M_n 9,000$	PAA average $M_n 9,000$	802190-1G	

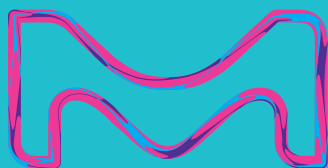
### Poly(lactide)-*block*-poly(5-methyl-5-allyloxycarbonyl-1,3-dioxan-2-one)

Name	Structure	Molecular Weight	Prod. No.
Poly(L-lactide- <i>co</i> -5-methyl-5-allyloxycarbonyl-1,3-dioxan-2-one)		$M_n 5,000$	795259-1G
		$M_n 10,000$	795267-1G
		$M_n 40,000$	792039-1G

# creative inking

Select. Formulate. **Bioprint.**

Want to keep innovation flowing in your bioprinting research? It's easy when you team up with a leader in polymers and nanomaterials for 3D printing. Watch your research take shape with our vast selection of materials and inks ready for your printer and application.

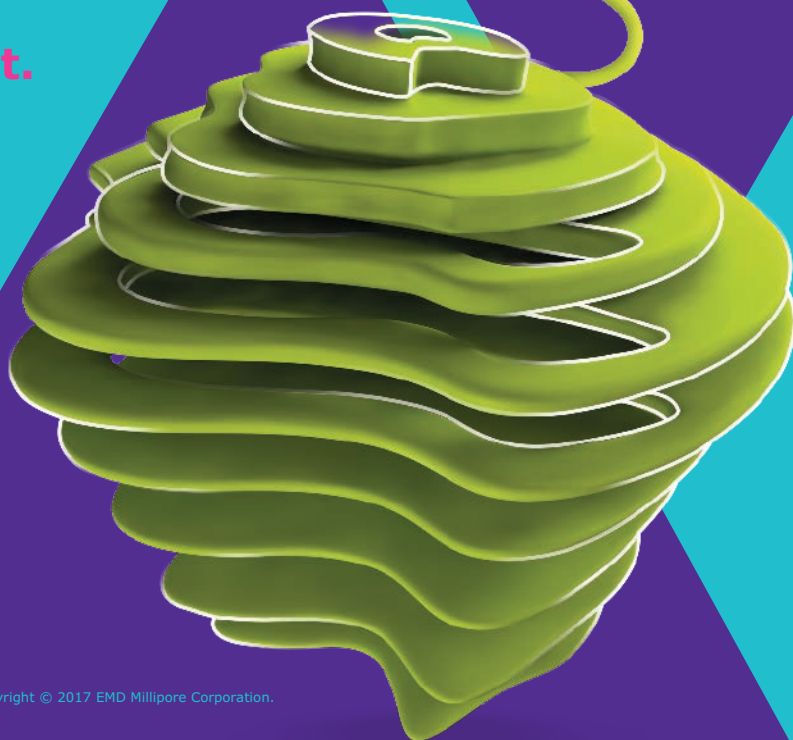


Discover more at  
[SigmaAldrich.com/3dp](http://SigmaAldrich.com/3dp)

The life science business of Merck KGaA, Darmstadt, Germany operates as MilliporeSigma in the U.S. and Canada.

MilliporeSigma and the vibrant M are trademarks of Merck KGaA, Darmstadt, Germany. Copyright © 2017 EMD Millipore Corporation. All Rights Reserved. 2017-01479

MILLIPORE  
SIGMA



# Protein- and Peptide-Polymer Conjugates by RAFT Polymerization



Matthias Hartlieb,<sup>1</sup> Raoul Peltier,<sup>1</sup> Sébastien Perrier<sup>1,2,3,\*</sup>

<sup>1</sup>Department of Chemistry, The University of Warwick, Coventry CV4 7AL, U.K.

<sup>2</sup>Warwick Medical School, The University of Warwick, Coventry CV4 7AL, U.K.

<sup>3</sup>Faculty of Pharmacy and Pharmaceutical Sciences, Monash University, VIC 3052, Australia

\*Email: s.perrier@warwick.ac.uk

## Introduction

The modification of biomacromolecules, such as peptides and proteins, through the attachment of synthetic polymers has led to a new family of highly advanced biomaterials with enhanced properties. These materials were first developed to enhance the circulation time of proteins *in vivo* through protection with covalently attached poly(ethylene glycol) (PEG), a process now commonly known as PEGylation. The conjugation of biomolecules to polymers has received a surge of interest over the last few years, triggered by new and versatile polymerization techniques that enable beneficial polymer functionalities and advanced material properties.

Polymer conjugates of biomolecules can be produced using either the convergent approach, in which the polymer is synthesized separately prior to conjugation with the biomolecule, or by the divergent methodology, in which the polymerization

reaction occurs in presence of the biomolecule (**Figure 1**).<sup>1</sup> The latter approach can be further divided into a grafting-from method, in which the biomolecule is functionalized with one or more units in order to grow a polymer chain, and a grafting-through method, in which the biomolecule is connected to a polymerizable unit that can be incorporated with other monomers to yield a bottle brush polymer decorated with biomolecules. Among the various polymerization techniques employed for the synthesis of these materials to date, reversible addition-fragmentation chain transfer (RAFT) polymerization has emerged as one of the most versatile and powerful processes. RAFT polymerization relies on a simple setup, versatile reaction conditions, and provides access to a myriad of functionalities, making it an ideal method for biomolecule modification.

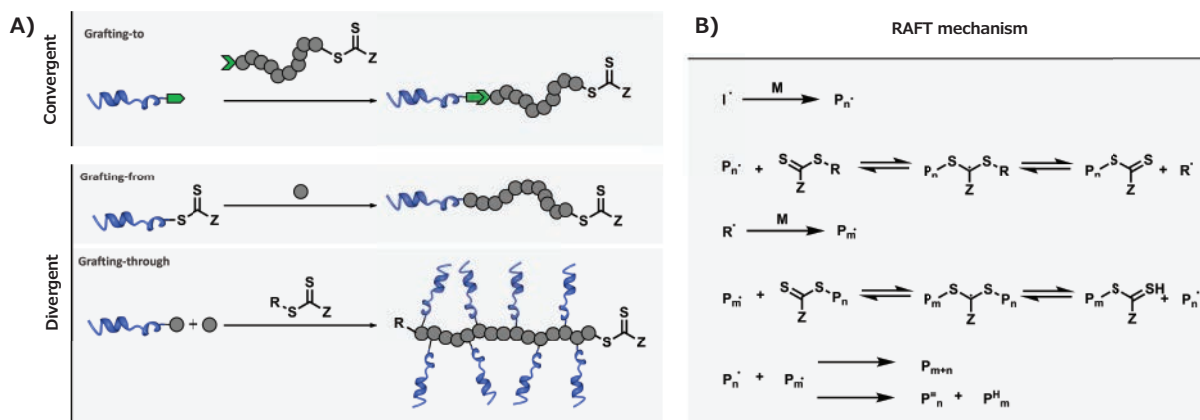


**Figure 1.** A) Possible strategies for the synthesis of peptide-polymer conjugates using a RAFT methodology. B) Mechanism of RAFT polymerization.

## Divergent Strategies to Peptide-Polymer Conjugates

The divergent approach has several specific advantages over convergent approaches for the synthesis of highly-defined, biomolecule-polymer conjugates. For example, the attachment of a small initiator molecule to the biomolecule allows for greater control compared to the conjugation of a polymeric chain, leading to better overall control over the number of polymers attached. In addition, purification is simplified since the removal of the polymeric species is not necessary.<sup>2</sup> However, the major disadvantage of the divergent approach is that the biomolecule must be compatible with the polymerization conditions, as it is involved in all synthetic steps.

RAFT polymerization is an ideal synthetic method for biomolecule-polymer conjugates because it is a robust and versatile process.<sup>3</sup> Radical polymerization processes are usually compatible with peptides or proteins since the propagating radical is non-reactive with the majority of functional groups associated with these biomolecules. Furthermore, RAFT polymerization enables polymerization of a wide range of monomers and does not require the use of a catalyst, avoiding the need for conjugate purification after the polymerization reaction. RAFT does require an external radical source, such as a thermal radical initiator (I), but the amount required is usually negligible especially in the case of high  $K_p$  monomers (e.g., acrylamides) allowing for high chain transfer agent/initiator (CTA/I) ratios to be used.<sup>4</sup>

As the divergent methodology requires biomolecule compatibility with polymerization conditions, polymer synthesis is ideally carried out in aqueous solution. RAFT is compatible with an aqueous environment and a large variety of hydrophilic monomers can be polymerized using water-soluble chain transfer agents (CTAs).<sup>5</sup> The reaction temperature must be kept low to reduce thermal degradation of the proteins or peptides during the polymerization process. This can be accomplished using a radical initiator with a low decomposition temperature (e.g., VA-044) or alternative radical sources, such as photoinitiators or suitable redox pairs.<sup>6</sup>

Another criteria to consider when using a divergent strategy in RAFT polymerization is CTA stability. Many RAFT agents (e.g., dithiobenzoates), are instable in the presence of nucleophiles, such as the primary amine of lysine, which are very commonly found in biomolecules. One strategy is the use of CTAs that are less sensitive to nucleophiles, such as trithiocarbonates. In addition, altering the solution pH during polymerization to ensure the protonation of a majority of amine functional

groups, enables the growth of RAFT-based polymers without interference from the protein. Free thiols found in proteins, such as those present in cysteine, can also interfere with RAFT-based polymerization processes as thiols can react irreversibly with a propagating radical and lead to the termination of a growing chain. In the case of synthetic peptides, protecting groups can be used and removed post-polymerization.

## RAFT-Based Grafting-From Methodology

To facilitate a grafting-from approach using RAFT polymerization, the CTA must be immobilized on the target peptide or protein, which can be performed via either the R- or Z-group (Figure 2).<sup>7</sup> If the R-group is utilized, the biomolecule acts as the initiator and the polymeric chain remains attached to the biomolecule throughout the entire process. While this method yields more stable conjugates, termination of a propagating radical leads to dead chains associated with the biomolecule, in which polymerization cannot be reinitiated.

If the CTA is attached via its Z-group, the polymer will grow in solution and reattach to the biomolecule (which carries the CTA) only during the chain transfer event. In this approach, a high livingness of the polymer attached to the biomolecule is achieved,<sup>8</sup> as dead chains will not reattach to the protein. However, especially in the case of long polymers, the reattachment step is sterically challenging, and can lead to a decrease in the number of polymer arms per biomolecule. In addition, the sensitivity of CTAs to nucleophiles renders Z-group conjugates comparably instable. While this instability may present issues in some applications, facile detachment of the polymer from the conjugate allows for ease of polymer analysis (e.g., size distribution).

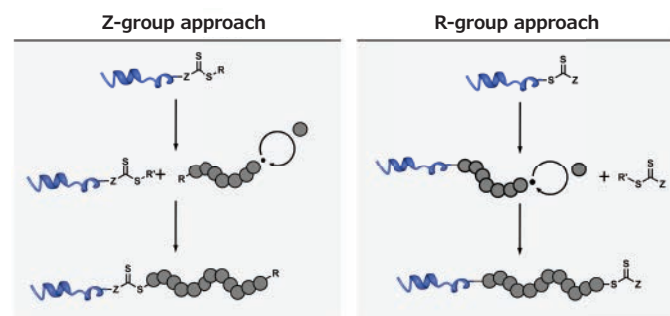


**Figure 2.** Comparison of the R- and Z-group approach using a RAFT-based grafting-from technique. The R'-leaving group of the chain transfer agent after the addition-fragmentation event has been omitted for clarity.

CTA molecules, such as dithiobenzoates or trithiocarbonates, are compatible with solid-phase peptide synthesis and can be attached to the *N*-terminus of a peptide on resin. After cleavage and polymerization, the peptide protecting groups are removed to yield the final conjugate.<sup>9,10</sup> Alternatively, the CTA can be attached to the pendant groups of peptides (e.g., glutathione or cyclic peptide nanotubes) as sites for polymer chain propagation.<sup>11,12</sup> RAFT-based, grafting-from approaches from proteins were demonstrated using BSA<sup>13</sup> and lysozyme,<sup>14</sup> utilizing either free thiol or amine groups and using either the R- or Z-group.<sup>15</sup> The preparation of block copolymer-based conjugates using this approach has also been described.<sup>16</sup>

### RAFT-Based Grafting-Through Methodology

The grafting-through approach requires functionalization of the peptide with a polymerizable group, such as an acrylate-based or styrene moiety, and is usually done as the last step of solid-phase peptide synthesis. These macromonomers can then be polymerized to yield densely peptide-functionalized polymers. This method has been used to create stimuli-responsive peptide brushes by incorporating  $\beta$ -sheet forming sequences.<sup>17,18</sup>

### Convergent Strategies to Peptide-Polymer Conjugates

A convergent, or grafting-to, approach is accomplished by reacting a specific protein site either to polymer pendant chains or to the RAFT agent at the chain end. Advantages of this method include the ability to use high temperature and organic solvents during the RAFT polymerization step, and easy characterization of the protein and polymer prior to coupling. In contrast, this approach requires high coupling efficiency and mild grafting conditions to retain protein activity. Due to the lack of diversity in naturally available functional groups on protein surfaces, reactions used in the grafting-to step were initially limited to reactions with amine and thiol groups. However, the introduction of unnatural amino acids via bioengineering techniques or post-translational modification procedures has drastically increased the number of conjugation techniques available.

### Conjugation Methods Using Amines

Primary amines (e.g.,  $\epsilon$ -amino group of lysine residues) are highly abundant on the surface of most proteins. The most common conjugation method for amine groups utilizes RAFT polymers modified with activated esters to form a stable and inert amide bond with the protein (**Figure 3**). Activated esters derived from *N*-hydroxysuccinimide (NHS, **Prod. No. 130672**) are often used due to mild coupling conditions and high coupling efficiency. For example, NHS derivatives of acrylic acid are

easily copolymerized with other monomers via RAFT, offering a convenient handle for post-polymerization modification. Controlling the ratio of NHS-bearing monomers incorporated in the polymer chain can be used to control the degree of protein-polymer functionalization.<sup>19</sup> While NHS groups feature facile conjugation chemistry, they also have a tendency to hydrolyze in aqueous solutions, and replacement with more stable alternatives, such as pentafluorophenyl methacrylate (**Prod. No. 741108**) is often a good option.<sup>20</sup> Alternatively, RAFT CTA containing activated esters can be used to graft a single protein at the end of the polymer chain. CTA containing  $\alpha$ -carboxylic acids can easily be converted into active esters through a reaction with NHS, either pre- or post-polymerization.<sup>21</sup> Protein conjugation can then be performed in slightly alkaline water or in DMSO with an organic base, such as *N,N*-diisopropylethylamine (**Prod. No. 496219**), to limit hydrolysis. Water-soluble, amide-promoting coupling agents (e.g., 1-ethyl-3-(3-dimethylaminopropyl)carbodiimide [EDC, **Prod. No. 39391**]) can also be used as an alternative to activated esters, directly reacting  $\alpha$ -carboxylic acids from RAFT polymers to free amine groups on proteins.<sup>22</sup> Additionally, particularly sensitive proteins, such as enzymes, can be coupled to RAFT polymers prepared using a CTA-bearing 2-mercaptothiazoline to create a biodegradable linker, allowing for the recovery of protein activity following linker cleavage.<sup>23</sup>

### Conjugation Methods Using Cysteines

Cysteine residues are far less abundant than lysine on the surface of biomacromolecules, reducing the risk of interference with the biological activity after polymer conjugation. The simplest method of functionalization is the formation of disulfide bonds, typically using activated disulfide residues, such as pyridyl disulfide (**Figure 3**). Again, two major approaches can be utilized. Pyridyl disulfide-bearing monomers, such as pyridyl disulfide methacrylamide, can be copolymerized using RAFT to yield copolymers that can be decorated with multiple copies of thiol-bearing proteins.<sup>24</sup> In contrast, a pyridyl disulfide-bearing CTA agent allows for the grafting of a single protein copy onto a polymer. For example, 3-(pyridin-2-yl-disulfanyl) propyl 2-(ethylthiocarbonothioylthio) propanoate was used to conjugate polymers to a variety of substrates ranging from glutathione to large proteins, such as basic fibroblast growth factors.<sup>25</sup> While disulfide bonds are useful for preparing bioresponsive systems, their sensitivity to reducing agents can lead to the premature cleavage of protein-polymer conjugates in some applications.

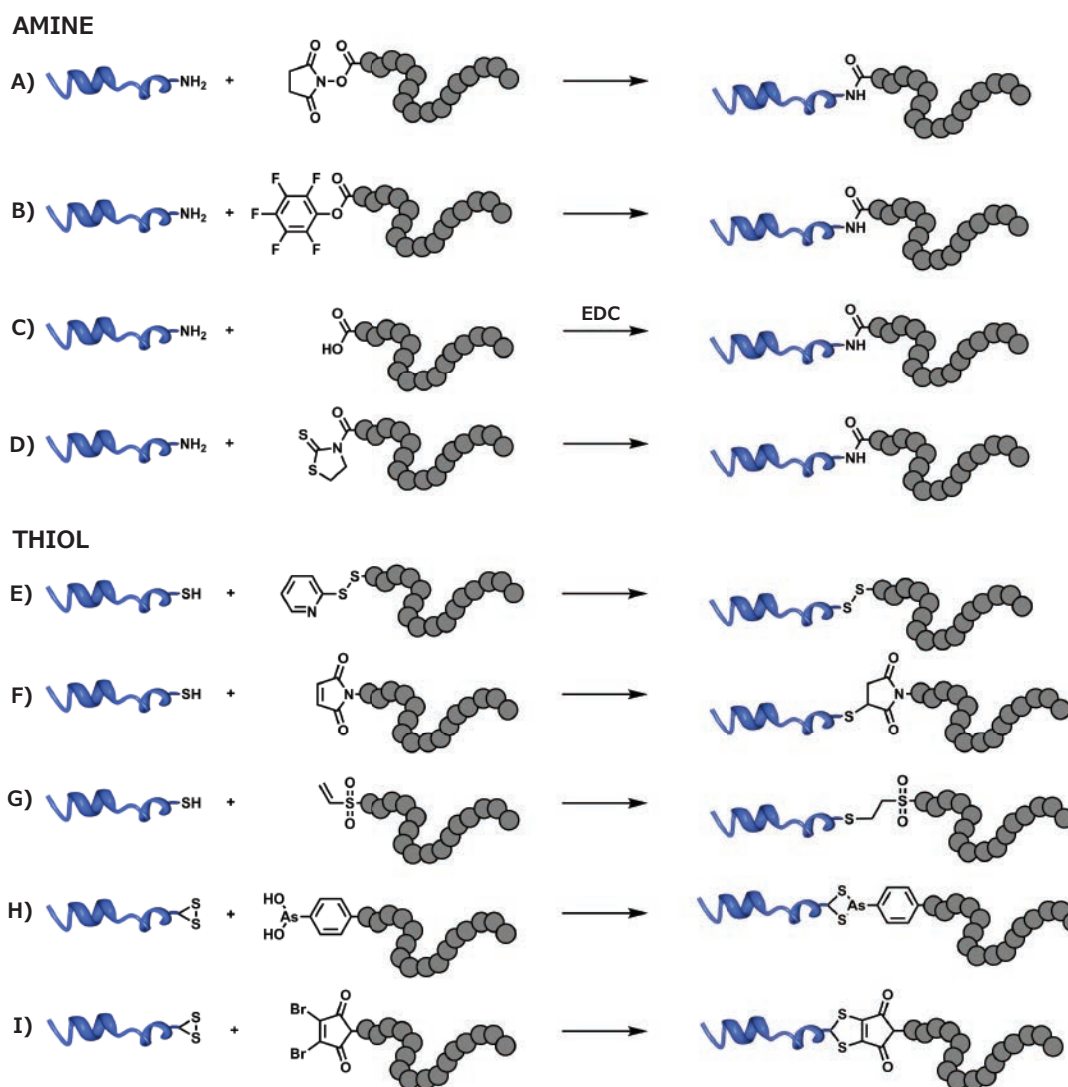


**Figure 3.** Conjugation of RAFT polymers to either lysine residues (amine) or cysteine residues (thiol) of proteins via A) reaction of an amine with an *N*-succinimidyl activated ester, B) reaction of an amine with a pentafluorophenyl activated ester, C) reaction of an amine with a carboxylic acid with EDC activation, D) reaction of an amine with a mercaptothiazoline ester, E) disulfide formation between a thiol and pyridyl disulfide, F) Michael addition of a thiol to a maleimide, G) Michael addition of a thiol to a vinyl sulfone, H) disulfide bridging using an arsenous acid, I) disulfide bridging using a dibromomaleimide.

A more stable alternative exploits the Michael addition of a thiol group to an  $\alpha$ - $\beta$  unsaturated carbonyl (e.g., maleimide or vinyl sulfone). RAFT polymers have been conjugated to bovine serum albumin (BSA) or ovalbumin using a 1,8-bis-maleimidodiethyleneglycol linker.<sup>26</sup> Another technique uses a CTA bearing a protected maleimide moiety for post-polymerization functionalization. For example, a furan-protected, maleimide-terminated analog of 4-cyanopentanoic acid dithiobenzoate (CPADB) was obtained in two steps from 10-dioxatricyclo[5.2.1.0<sub>2,6</sub>]dec-8-ene-3,5-dione and used to prepare maleimide-terminated poly(methyl methacrylate) (PMMA). This functionalized polymer was subsequently

conjugated to albumin by simply stirring in PBS buffer.<sup>27</sup> To avoid the protection and deprotection cycle, the  $\alpha$ - $\beta$  unsaturated carbonyl moiety can be added to the polymer after the polymerization step.<sup>28</sup>

Enhanced specificity can be obtained by targeting native disulfide bonds in proteins instead of isolated thiol residues. This has been successfully achieved using a trivalent derivative of arsenous acid and RAFT polymerization.<sup>29</sup> The use of dibromomaleimide functional groups, however, has only been used in conjunction with atom transfer radical polymerization (ATRP) and remains to be implemented with a RAFT-made polymer.<sup>30</sup>



## Conjugation Methods Using Unnatural Amino Acids

To achieve site-selective ligation, a range of bioorthogonal reactions have been developed that utilize unnatural amino acids (UAA). While incorporation of UAA in a peptide sequence can be easily achieved via solid-phase peptide synthesis, UAA incorporation in proteins requires either post-translational modification or genetically encoding UAA incorporation during bacterial expression.<sup>31</sup>

“Click” reactions, such as copper(I)-mediated azide-alkyne cycloaddition (CuAAC), are perfectly suited for bioconjugation as they feature orthogonal reactivity to biological functional groups, high conversion, limited side reactions, and compatibility with aqueous conditions. Using (prop-2-ynyl propanoate)yl butyltrithiocarbonate as the CTA, Perrier et al. prepared alkyne-terminated RAFT polymers that were later coupled to a peptide

bearing an azide functional group (Figure 4).<sup>32</sup> The reverse can also be synthesized by ligating an azido-bearing polymer to a protein in which a cysteine was modified with propargyl maleimide.<sup>33</sup> This reaction, however, has several disadvantages including the lack of full conversion without microwave irradiation and the use of a toxic copper catalyst, which could interfere with subsequent biological applications. A more biocompatible approach uses strained cycloalkynes or cycloalkenes that can react with azides or tetrazines, respectively, in the absence of copper catalyst. A maleimide-*trans*-cyclooctene linker was used to modify the cysteine residue of a lysozyme protein mutant, and later used to couple two copies of the protein to a tetrazine-bearing polymer.<sup>34</sup> Strained alkynes can also be attached to the CTA prior to RAFT polymerization. For example, poly-*N*-(2-hydroxypropyl)methacrylamide (PHPMA) polymerized using an  $\alpha$ -dibenzocyclooctyne-containing CTA was directly conjugated to an azide-modified peptide, after polymerization.<sup>35</sup>

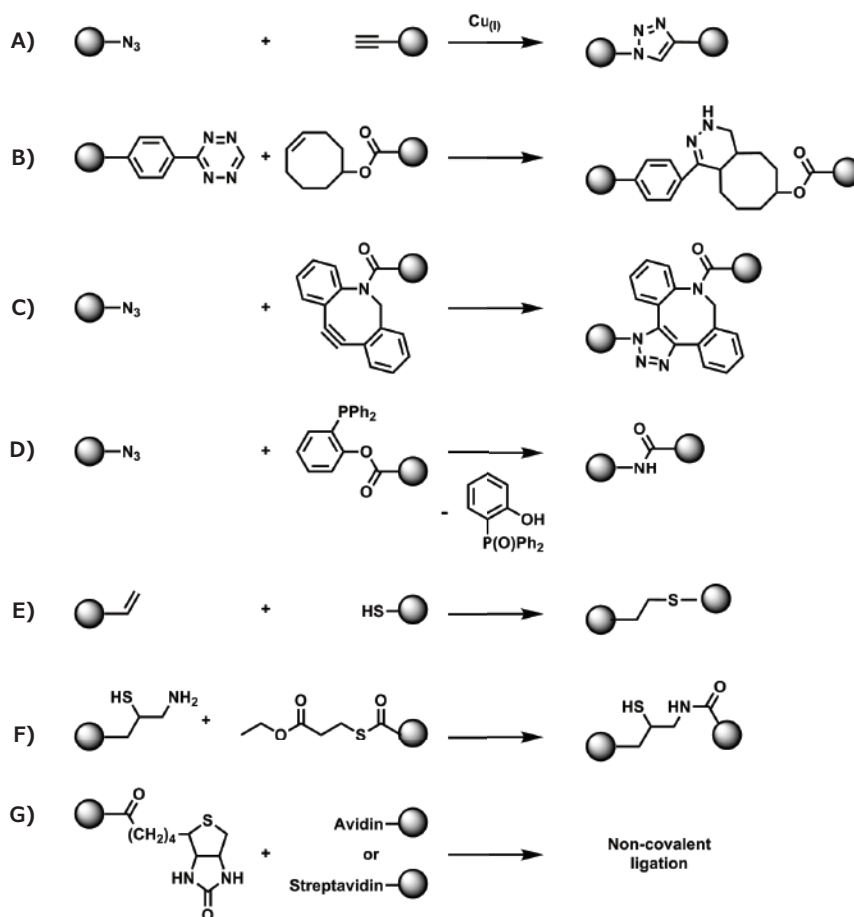


**Figure 4.** Conjugation of RAFT polymers to non-naturally occurring functional group of proteins via **A)** copper(I)-mediated azide-alkyne cycloaddition, **B)** metal-free tetrazine-*trans*-cyclooctene ligation, **C)** metal-free ligation of dibenzocyclooctyne to an azide, **D)** Staudinger ligation of an azide with a phosphine, **E)** thiol-ene ligation, **F)** native chemical ligation of a thioester to a terminal cysteine, **G)** non-covalent ligation based on affinity of biotin with avidin or streptavidin. The spheres in this scheme are interchangeable and can represent either the polymer or the protein molecules.

As a highly specific reaction, a Staudinger ligation is used to bind an azide selectively to a phosphine group. For RAFT applications, the phosphine can be introduced to the  $\alpha$ -carboxylic acid of common CTAs via reaction with 2-(diphenylphosphanyl)phenol<sup>36</sup> allowing for quantitative ligation to azide-containing macromolecules in an aqueous environment. For shorter peptides, thiol-ene click chemistry can be exploited to couple an allyl oxycarbonyl-protected lysine residue to a RAFT-synthesized polymer, which had undergone aminolysis.<sup>37</sup> Native chemical ligation can also be used to conjugate a peptide thioester to a RAFT polymer modified to incorporate a single pseudo-cysteine monomer.<sup>38</sup>

Finally, an elegant way to conjugate polymers and proteins exploits the inherent affinity of biotin, a co-factor involved in multiple eukaryotic biological processes, to avidin or streptavidin proteins. Due to its relatively small size, biotin can easily be introduced onto a CTA prior to RAFT polymerization.<sup>39</sup>

Additional information about common grafting-to methods can be found in the a recent, comprehensive article by Vanparijs et al.<sup>40</sup> New directions in protein-polymer conjugates synthesis have exploited orthogonal combinations of these reactions to generate more advanced materials by attaching different proteins to the same polymer. For example, Maynard et al. successfully prepared a poly-NIPAM polymer utilizing a dual functional RAFT chain transfer agent to yield a polymer with biotin on one end and a maleimide group on the other.<sup>41</sup>

## Conclusion

The versatility of the RAFT process has made it an ideal tool for the modification of biomolecules, particularly peptides and proteins. RAFT not only enables the introduction of functional groups and novel properties to peptide and proteins, but also the versatility of the process permits a flexible synthetic approach for bioconjugates. With a large variety of established synthetic techniques now available, complex conjugate structures have created a path for a wealth of applications in a variety of fields.

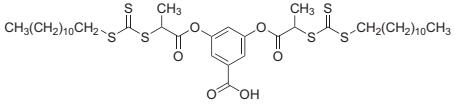
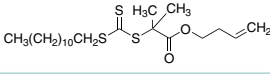
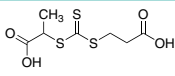
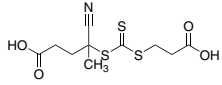
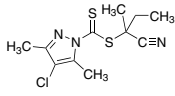
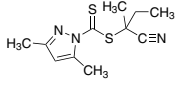
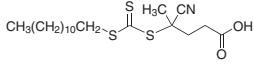
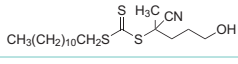
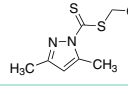
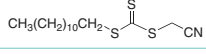
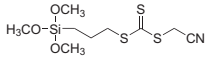
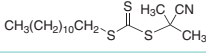
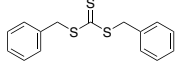
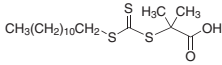
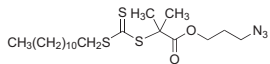
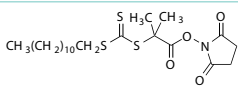
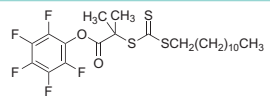
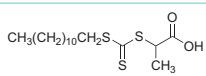
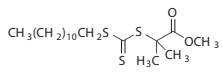
## References

- (1) Dehn, S.; Chapman, R.; Jolliffe, K. A.; Perrier, S. *Polym. Rev.* **2011**, *51*, 214.
- (2) Bulmus, V. *Polym. Chem.* **2011**, *2*, 1463.
- (3) Cobo, I.; Li, M.; Sumerlin, B. S.; Perrier, S. *Nat Mater* **2015**, *14*, 143.
- (4) Gody, G.; Barbey, R.; Danial, M.; Perrier, S. *Polym. Chem.* **2015**, *6*, 1502.
- (5) Lowe, A. B.; McCormick, C. L. *Prog. Polym. Sci.* **2007**, *32*, 283.
- (6) Martin, L.; Gody, G.; Perrier, S. *Polym. Chem.* **2015**, *6*, 4875.
- (7) Sumerlin, B. S. *ACS Macro Lett.* **2012**, *1*, 141.
- (8) Gody, G.; Maschmeyer, T.; Zetterlund, P. B.; Perrier, S. *Macromolecules* **2014**, *47*, 639.
- (9) Hentschel, J.; Bleek, K.; Ernst, O.; Lutz, J.-F.; Börner, H. G. *Macromolecules* **2008**, *41*, 1073.
- (10) ten Cate, M. G. J.; Rettig, H.; Bernhardt, K.; Börner, H. G. *Macromolecules* **2005**, *38*, 10643.
- (11) Zhao, Y.; Perrier, S. *Chem. Commun.* **2007**, *41*, 4294.
- (12) Larnaudie, S. C.; Brendel, J. C.; Jolliffe, K. A.; Perrier, S. *J. Polym. Sci., Part A: Polym. Chem.* **2015**, *54*(7), 1003-1011.
- (13) De, P.; Li, M.; Gondi, S. R.; Sumerlin, B. S. *J. Am. Chem. Soc.* **2008**, *130*, 11288.
- (14) Li, H.; Bapat, A. P.; Li, M.; Sumerlin, B. S. *Polym. Chem.* **2011**, *2*, 323.
- (15) Boyer, C.; Bulmus, V.; Liu, J.; Davis, T. P.; Stenzel, M. H.; Barner-Kowollik, C. *J. Am. Chem. Soc.* **2007**, *129*, 7145.
- (16) Li, H.; Li, M.; Yu, X.; Bapat, A. P.; Sumerlin, B. S. *Polym. Chem.* **2011**, *2*, 1531.
- (17) Fernández-Trillo, F.; Duréault, A.; Bayley, J. P. M.; van Hest, J. C. M.; Thies, J. C.; Michon, T.; Weberskirch, R.; Cameron, N. R. *Macromolecules* **2007**, *40*, 6094.
- (18) Kumar, S.; Bheemireddy, V.; De, P. *Macromol. Biosci.* **2015**, *15*, 1447.
- (19) Peng, H.; Kather, M.; Rubsam, K.; Jakob, F.; Schwaneberg, U.; Pich, A. *Macromolecules* **2015**, *48*, 4256.
- (20) Roy, D.; Nehilla, B. J.; Lai, J. J.; Stayton, P. S. *ACS Macro Lett.* **2013**, *2*, 132.
- (21) Danial, M.; Tran, C. M. N.; Jolliffe, K. A.; Perrier, S. *J. Am. Chem. Soc.* **2014**, *136*, 8018.
- (22) Falatach, R.; Li, S. H.; Sloane, S.; McGlone, C.; Berberich, J. A.; Page, R. C.; Averick, S.; Konkolewicz, D. *Polymer* **2015**, *72*, 382.
- (23) Liu, H. H.; Zhang, J. Z.; Luo, X.; Kong, N.; Cui, L.; Liu, J. Q. *Eur. Polym. J.* **2013**, *49*, 2949.
- (24) Crownover, E. F.; Convertine, A. J.; Stayton, P. S. *Polym. Chem.* **2011**, *2*, 1499.
- (25) Nguyen, T. H.; Kim, S. H.; Decker, C. G.; Wong, D. Y.; Loo, J. A.; Maynard, H. D. *Nat. Chem.* **2013**, *5*, 221.
- (26) Li, M.; De, P.; Li, H. M.; Sumerlin, B. S. *Polym. Chem.* **2010**, *1*, 854.
- (27) Jiang, Y. Y.; Lu, H. X.; Khine, Y. Y.; Dag, A.; Stenzel, M. H. *Biomacromolecules* **2014**, *15*, 4195.
- (28) Grover, G. N.; Alconcel, S. N. S.; Matsumoto, N. M.; Maynard, H. D. *Macromolecules* **2009**, *42*, 7657.
- (29) Footman, C.; de Jongh, P. A. J. M.; Tanaka, J.; Peltier, R.; Kempe, K.; Davis, T. P.; Wilson, P. *Chem. Commun.* **2017**, *53*, 8447.
- (30) Wilson, P.; Anastasaki, A.; Owen, M. R.; Kempe, K.; Haddleton, D. M.; Mann, S. K.; Johnston, A. P. R.; Quinn, J. F.; Whittaker, M. R.; Hogg, P. J.; Davis, T. P. *J. Am. Chem. Soc.* **2015**, *137*, 4215.
- (30) Connor, R. E.; Tirrell, D. A. *Polym. Rev.* **2007**, *47*, 9.
- (31) Chapman, R.; Warr, G. G.; Perrier, S.; Jolliffe, K. A. *Chem. Eur. J.* **2013**, *19*, 1955.
- (32) Li, M.; De, P.; Gondi, S. R.; Sumerlin, B. S. *Macromol. Rapid Commun.* **2008**, *29*, 1172.
- (33) Lorenzo, M. M.; Decker, C. G.; Kahveci, M. U.; Paluck, S. J.; Maynard, H. D. *Macromolecules* **2016**, *49*, 30.
- (34) Pola, R.; Braunova, A.; Laga, R.; Pechar, M.; Ulbrich, K. *Polym. Chem.* **2014**, *5*, 1340.
- (35) Potzsch, R.; Fleischmann, S.; Tock, C.; Komber, H.; Voit, B. I. *Macromolecules* **2011**, *44*, 3260.
- (36) Danial, M.; Tran, C. M.-N.; Young, P. G.; Perrier, S.; Jolliffe, K. A. *Nat. Commun.* **2013**, *4*, 2780.
- (37) Isahak, N.; Gody, G.; Malins, L. R.; Mitchell, N. J.; Payne, R. J.; Perrier, S. *Chem. Commun.* **2016**, *52*, 12952.
- (38) Hong, C. Y.; Pan, C. Y. *Macromolecules* **2006**, *39*, 3517.
- (39) Vanparijs, N.; Maji, S.; Louage, B.; Voorhaar, L.; Laplace, D.; Zhang, Q.; Shi, Y.; Hennink, W. E.; Hoogenboom, R.; De Geest, B. G. *Polym. Chem.* **2015**, *6*, 5602.
- (40) Heredia, K. L.; Grover, G. N.; Tao, L.; Maynard, H. D. *Macromolecules* **2009**, *42*, 2360.

## RAFT Agents

For a complete list of available materials, visit [SigmaAldrich.com/raftagent](http://SigmaAldrich.com/raftagent).

### Trithiocarbonates

Name	Structure	Purity	Prod. No.
3,5-Bis(2-dodecylthiocarbonothioylthio)-1-oxopropoxy)benzoic acid		98%, HPLC	763071-1G 763071-5G
3-Butenyl 2-(dodecylthiocarbonothioylthio)-2-methylpropionate		97%	768723-1G
2-(2-Carboxyethylsulfanylthiocarbonyl-sulfanyl)propionic acid		95%, GC	900152-1G
4-(((2-Carboxyethyl)thio)carbonothioyl)thio)-4-cyanopentanoic acid		95%	900161-1G
2-Cyanobutan-2-yl 4-chloro-3,5-dimethyl-1H-pyrazole-1-carbodithioate		95%	900158-1G
2-Cyanobutan-2-yl 3,5-dimethyl-1H-pyrazole-1-carbodithioate		95%	900157-1G
4-Cyano-4-[(dodecylsulfanylthiocarbonyl)sulfanyl]pentanoic acid		97%, HPLC	723274-1G 723274-5G
4-Cyano-4-[(dodecylsulfanylthiocarbonyl)sulfanyl]pentanol		≥96.5%, HPLC	760110-1G 760110-5G
Cyanomethyl (3,5-Dimethyl-1H-pyrazole)-carbodithioate		95%	900150-1G
Cyanomethyl dodecyl trithiocarbonate		98%, HPLC	723029-1G 723029-5G
Cyanomethyl [3-(trimethoxysilyl)propyl]trithiocarbonate		95%, GC	773808-1G
2-Cyano-2-propyl dodecyl trithiocarbonate		97%, HPLC	723037-1G 723037-5G
S,S-Dibenzyl trithiocarbonate		97%	746304-1G 746304-5G
2-(Dodecylthiocarbonothioylthio)-2-methylpropionic acid		98%, HPLC	723010-1G 723010-5G
2-(Dodecylthiocarbonothioylthio)-2-methylpropionic acid 3-azido-1-propanol ester		98%, HPLC	741698-1G 741698-5G
2-(Dodecylthiocarbonothioylthio)-2-methylpropionic acid N-hydroxysuccinimide ester		98%, HPLC	741035-1G 741035-5G
2-(Dodecylthiocarbonothioylthio)-2-methylpropionic acid pentafluorophenyl ester		-	740810-1G 740810-5G
2-(Dodecylthiocarbonothioylthio)propionic acid		97%	749133-1G 749133-5G
Methyl 2-(dodecylthiocarbonothioylthio)-2-methylpropionate		97%, HPLC	740497-1G 740497-5G

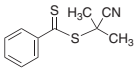
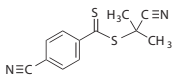
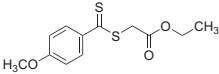
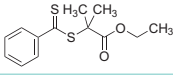
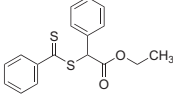
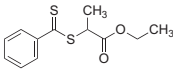
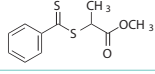
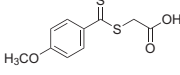
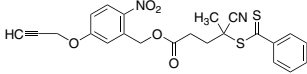
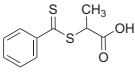
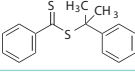
Name	Structure	Purity	Prod. No.
Pentaerythritol tetrakis[2-(dodecylthiocarbonothioylthio)-2-methylpropionate]		97%, HPLC	763551-1G
Phthalimidomethyl butyl trithiocarbonate		97%	777072-1G
1,1,1-Tris[(dodecylthiocarbonothioylthio)-2-methylpropionate]ethane		98%, HPLC	763543-1G

## Dithiocarbonates

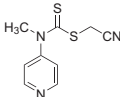
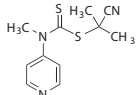
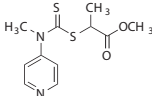
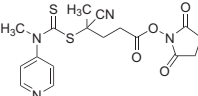
Name	Structure	Purity	Prod. No.
Benzyl 1H-pyrrole-1-carbodithioate		97%, HPLC	753106-1G 753106-5G
Cyanomethyl diphenylcarbomodithioate		97%, HPLC	751200-1G 751200-5G
Cyanomethyl methyl(phenyl) carbomodithioate		98%, HPLC	723002-1G 723002-5G
Cyanomethyl methyl(4-pyridyl) carbomodithioate		98%	738689-1G 738689-5G
2-Cyanopropan-2-yl <i>N</i> -methyl- <i>N</i> -(pyridin-4-yl)carbomodithioate		97%, HPLC	736236-1G 736236-5G
Methyl 2-[methyl(4-pyridyl) carbomothioylthio]propionate		97%	735639-1G 735639-5G
1-Succinimidyl-4-cyano-4-[ <i>N</i> -methyl- <i>N</i> -(4-pyridyl)carbomothioylthio]pentanoate		98%, HPLC	751227-1G

## Dithiobenzoates

Name	Structure	Purity	Prod. No.
Benzyl benzodithioate		96%	760439-1G 760439-5G
Cyanomethyl benzodithioate		98%, HPLC	763500-1G
4-Cyano-4-(phenylcarbonothioylthio) pentanoic acid		>97%	722995-1G 722995-5G
4-Cyano-4-(phenylcarbonothioylthio) pentanoic acid <i>N</i> -succinimidyl ester		-	758353-1G

Name	Structure	Purity	Prod. No.
2-Cyano-2-propyl benzodithioate		>97%, HPLC	722987-1G 722987-5G
2-Cyano-2-propyl 4-cyanobenzodithioate		98%, HPLC	731277-1G 731277-5G
Ethyl 2-(4-methoxyphenylcarbonothioylthio)acetate		99%	774472-1G
Ethyl 2-methyl-2-(phenylthiocarbonylthio)propionate		95%	741701-1G
Ethyl 2-(phenylcarbonothioylthio)-2-phenylacetate		98%	773506-1G
Ethyl 2-(phenylcarbonothioylthio)propionate		97%, HPLC	760455-1G
1-(Methoxycarbonyl)ethyl benzodithioate		≥97%	751138-1G
2-(4-Methoxyphenylcarbonothioylthio)ethanoic acid		≥97%	775886-1G
2-Nitro-5-(2-propynyloxy)benzyl 4-cyano-4-(phenylcarbonothioylthio)pentanoate		97%	765147-1G
2-(Phenylcarbonothioylthio)propanoic acid		98%	773778-1G
2-Phenyl-2-propyl benzodithioate		99%, HPLC	731269-1G 731269-5G

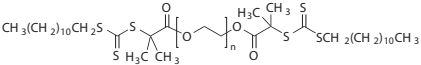
## Switchable RAFT Agents

Name	Structure	Purity	Prod. No.
Cyanomethyl methyl(4-pyridyl) carbamodithioate		98%	738689-1G 738689-5G
2-Cyanopropan-2-yl <i>N</i> -methyl- <i>N</i> -(4-pyridin-4-yl)carbamodithioate		97%, HPLC	736236-1G 736236-5G
Methyl 2-[methyl(4-pyridinyl) carbamothioylthio]propionate		97%	735639-1G 735639-5G
1-Succinimidyl-4-cyano-4-[ <i>N</i> -methyl- <i>N</i> -(4-pyridyl)carbamothioylthio]pentanoate		98%, HPLC	751227-1G

## Macro-RAFT Agents

For a complete list of available materials, visit [SigmaAldrich.com/raftagent](http://SigmaAldrich.com/raftagent).

## Poly(ethylene glycol)-Based

Name	Structure	Molecular Weight (PEG)	Polydispersity	Prod. No.
Poly(ethylene glycol) bis[2-(dodecylthiocarbonylthio)-2-methylpropionate]		average $M_n$ 10,800	≤ 1.1	753025-1G

Name	Structure	Molecular Weight (PEG)	Polydispersity	Prod. No.
Poly(ethylene glycol) 4-cyano-4-(phenylcarbonothioylthio)pentanoate		average $M_n$ 10,000	$\leq 1.1$	764930-1G
		average $M_n$ 2,000	$\leq 1.1$	764914-1G
Poly(ethylene glycol) methyl ether [(dodecylsulfanylthiocarbonyl) sulfanyl]pentanoate		average $M_n$ 10,000	$\leq 1.1$	753033-1G
Poly(ethylene glycol) methyl ether (4-cyano-4-pentanoate dodecyl trithiocarbonate)		average $M_n$ 5,400	$\leq 1.1$	751626-1G 751626-5G
		average $M_n$ 2,400	$\leq 1.1$	751634-1G 751634-5G
		average $M_n$ 1,400	$\leq 1.1$	752487-1G 752487-5G
Poly(ethylene glycol) methyl ether 2-(dodecylthiocarbonothioylthio)-2-methylpropionate		average $M_n$ 5,000	$\leq 1.1$	736325-1G
		average $M_n$ 1,100	$\leq 1.1$	740705-1G
Poly(ethylene glycol) methyl ether (2-methyl-2-propionic acid dodecyl trithiocarbonate)		average $M_n$ 10,000	$\leq 1.1$	752495-1G

## Poly(styrene)-Based

Name	Structure	Molecular Weight	Polydispersity	Prod. No.
Poly(styrene), DDMAT terminated		10,000	$\leq 1.1$	772569-1G
		5,000	$< 1.1$	772577-1G

## Poly(lactide)-Based

Name	Structure	Molecular Weight	Polydispersity	Prod. No.
Poly(D,L-lactide), 4-cyano-4-[(dodecylsulfanylthiocarbonyl) sulfanyl]pentanoate terminated		average $M_n$ 20,000	$< 1.4$	797790-1G
		average $M_n$ 10,000	$< 1.4$	797804-1G
Poly(L-lactide) 4-cyano-4-[(dodecylsulfanylthiocarbonyl) sulfanyl]pentanoate		$M_n$ 10,000	$\leq 1.2$	746533-1G
		average $M_n$ 5,000	$\leq 1.2$	746525-1G
Poly(D,L-lactide), 4-cyano-4-[(dodecylsulfanylthiocarbonyl) sulfanyl]pentanoate terminated		average $M_n$ 5000	$\leq 1.5$	792020-1G

## Poly(acrylate)-Based

Name	Structure	Molecular Weight	Polydispersity	Prod. No.
Poly(acrylic acid), DDMAT terminated		10,000	$\leq 1.1$	775843-1G
Poly( <i>tert</i> -butyl acrylate), DDMAT terminated, azide terminated		8,500	$\leq 1.2$	776424-1G
Poly( <i>tert</i> -butyl acrylate), DDMAT terminated		7,000	$< 1.2$	772550-1G
Poly(hydroxyethyl methacrylate), DDMAT terminated		7,000	$< 1.2$	772542-1G

## Poly(acrylamide)-Based

Name	Structure	Molecular Weight	Polydispersity	Prod. No.
Poly( <i>N,N</i> -dimethylacrylamide), DDMAT terminated		10,000	$\leq 1.1$	773638-1G

# Functionalized PEI and Its Role in Gene Therapy



Bettina Schwarz,<sup>1</sup> Olivia M. Merkel<sup>1,2\*</sup>

<sup>1</sup>Department of Pharmacy, Pharmaceutical Technology and Biopharmacy, Ludwig-Maximilians-Universität München, Butenandtstraße 5, 81377 München, Germany

<sup>2</sup>Nanosystems Initiative Munich (NIM), Ludwig-Maximilians-Universität München, Schellingstraße 4, 80799 München, Germany

\*Email: Olivia.merkel@lmu.de

## Introduction

Gene therapy has become one of the most discussed techniques in biomedical research in recent years. Gene therapy is the treatment of a variety of diseases and genetic disorders by delivering genetic materials into cells. However, success of this treatment method is still limited due to the lack of safe and efficient carrier systems.

Poly(ethyleneimine) (PEI) has been extensively explored as a state-of-art gene carrier for *in vitro* and *in vivo* applications. PEI readily forms polyplexes with nucleic acids via electrostatic self-assembly. Polyplexes provide superior transfection efficiency due to the high buffering capacity of PEI, which is beneficial for endosomal escape of the gene payload.<sup>1</sup> Despite these advantages, PEI is not degradable, lacks specificity, yields inherently instable complexes, and aggregates in the blood, resulting in high toxicity. There has been a significant focus on the modification of PEI and its corresponding effects on gene delivery. While low molecular weight PEI has been shown to be less cytotoxic *in vivo* than high molecular weight derivatives,<sup>2</sup> low molecular weight PEI results in reduced transfection efficiency. Based upon these results, current research has focused on the design of degradable PEI derivatives using low molecular weight PEI and a variety of crosslinkers. Moreover, different polymers and ligands have been used to increase transfection efficiency and target specificity.

This review focuses on current advancements in the development of modified PEI derivatives as gene carriers for small interfering RNA (siRNA) and DNA and briefly describes different chemical modifications of PEI supported by *in vivo* results. Topics covered include PEI-coupled polymers to enhance polyplex stability, transfection efficiency, and the addition of targeting ligands and biodegradable linkages.

## Modifications of PEI by Polymer Functionalization

Despite its unique properties, unmodified PEI suffers from cytotoxicity, lack of biodegradability, poor transfection efficiency of low molecular weight homologues, and insufficient target

specificity. To obtain more efficient non-viral vectors for gene delivery, a substantial focus has been placed on PEI modifications in the last several years. Polymers, ligands, and chemical modifications have been used to improve the physicochemical properties of PEI, as well as enhance its biocompatibility and transfection efficiency. The modification of PEI with polymers to enhance transfection efficiency has attracted significant interest and utilizes a wide variety of polymers including oligosaccharides, poly(ethylene glycol) (PEG), poly( $\epsilon$ -caprolactone), and others. The most common and recent modifications are described briefly herein.

## PEG

One of the first and most extensively investigated PEI modifications is the covalent coupling of poly(ethylene glycol) (PEG) (**Figure 1**). Since PEG is non-ionic and water-soluble, conjugation with PEG improves biocompatibility, reduces cytotoxicity, and increases circulation time *in vivo*.<sup>3</sup> Mao et. al<sup>4</sup> found that both the chain length and graft density of PEG strongly influence siRNA condensation and polyplex stability *in vitro*. While a tremendous number of studies have been performed *in vitro*, *in vivo* experiments showing the effects of PEG-PEI/siRNA complexes are essential for the validation of new materials. Merkel et al.<sup>5</sup> investigated the delivery of PEG-PEI polyplexes to the lungs of mice. Preliminary *in vitro* results suggested PEI/siRNA without PEG had the least immunogenicity and best stability, but these results were not supported by subsequent *in vivo* knockdown experiments. In the secondary experiments, PEG-PEI/siRNA complexes showed higher stability and elevated immune responses but no histological abnormalities, while unmodified PEI/siRNA complexes deposited PEI in the lungs and released the siRNA payload too early.

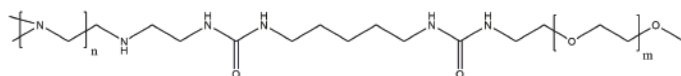


**Figure 1.** Example structure of a PEI modification with PEG.

## Saccharides

Due to its biodegradability, biocompatibility, and low toxicity, chitosan is the most common polysaccharide used for grafting on PEI. To overcome its poor transfection efficiency, modified derivatives such as glycol chitosan have been attached to PEI polymers.<sup>6</sup> This gene carrier reduces the cytotoxicity of PEI while enhancing endosomal escape and GFP transfection efficacy in HEK 293 cells. Apart from polysaccharides, oligosaccharides are frequently used to alter the pharmacokinetic properties of PEI. Gutsch et al.<sup>7</sup> examined a set of different oligomaltose-PEI-based DNA and siRNA complexes for their biocompatibility and efficacy *in vivo*. They found oligomaltose-grafted PEI increases DNA delivery efficiency, decreases weight loss, abrogates hepatotoxicity, and abolishes lethality in mice in the study when compared to free polymers. Another interesting approach is the use of cellulose nanocrystals (CNCs) as vehicles for siRNA delivery.<sup>8</sup> These rodlike nanoparticles feature biodegradability, lack of cytotoxicity, and enhanced cellular uptake. In a recent report, CNCs were coated with a covalently-attached, cationic PEI shell capable of binding siRNA via electrostatic interactions. This new nanocarrier showed no cytotoxicity and good transfection efficiency compared to a commercial transfection reagent *in vitro*.

## Poly lactide

To increase hydrophobicity for better cell penetration and overall biodegradability, Abebe et al.<sup>9</sup> designed triblock copolymers constituted of linear PEI, PEG, and poly(L-lactide) (PLLA). They prepared multi-layered micelles with PLLA-PEI-PLLA as the hydrophobic core encapsulating the genetic material and PLLA-PEG-PLLA as the outer shell to ensure stability in aqueous suspensions. The resulting micelles show low cytotoxicity and high stability at neutral pH, but the outer shell was easily destabilized in acidic conditions, releasing the nucleic acids immediately.

## Other Polymers

There are numerous other ways to modify PEI with different copolymers to yield better transfection efficiencies and reduced cytotoxicity. A multifunctional, cationic triblock copolymer based on PEG, poly( $\epsilon$ -caprolactone) (PCL), and PEI was designed for the delivery of siRNA.<sup>10</sup> The hydrophobic PCL domain increased the affinity for the cell membrane, maintaining better internalization. Since this layer can also serve as a reservoir for hydrophobic substances, the system has the potential to be used for the simultaneous delivery of nucleic acids and hydrophobic drugs or dyes. These hydrophobic, amphiphilic nanocarriers showed superior transfection efficiency when delivered to the lungs of BALB/c mice via inhalation. PEI conjugates of single-walled carbon nanotubes can also be used to reduce PEI's cytotoxicity while enhancing its transfection efficiency.<sup>11</sup>

This nanovector takes advantage of both the morphology-based, needle-effect cell penetration of carbon nanotubes and the endosomal escape ability of PEI. In addition to the enhanced transfection efficiency and low cytotoxicity, disulfide linkages were incorporated to impart biodegradability into the nanoconstruct. In comparison to 25 kDa PEI, the nanocarriers showed greater than 800-fold higher transfection levels *in vitro*.

## Ligand-Modified PEI

An ideal gene delivery system should deliver intact nucleic acids without side effects, while also providing a basis for cell- or tissue-specific targeting. Many *in vivo* studies have demonstrated the inability of genetic material to enter the cell nucleus. To overcome this drawback and enhance targeting efficiency of PEI-based polyplexes, the polymer must be modified with distinct targeting ligands. Many different approaches have been reported; only select reactions will be described here.

## Peptides

Specific peptide sequences that interact with receptors expressed predominantly by tumor cells can be included to facilitate cell and nucleus penetration. Hu et al.<sup>12</sup> designed a PEI-based vector modified with the trifunctional peptide R18, which contains TAT (a cell penetrating peptide), RGDC (a cell adhesive peptide), and a nuclear localization sequence (NLS), to increase the nuclear import of genetic material. This nanovector showed controlled degradation, high buffer capabilities, and low cytotoxicity. Confocal fluorescence microscopy confirmed accumulation in the nucleus after cellular uptake. In addition, *in vivo* results in mice support the importance of the NLS fragment to increase the efficiency of nuclear transfection, compared to the complex without the NLS sequence or any peptide modification.

## Neutralization of Surface Charge

The neutralization of PEI surface charge has been shown to increase biocompatibility and enhance cell internalization efficiency.<sup>13</sup> Substitution of the primary amines of PEI with hydrazide groups was shown to allow for further modification with targeting ligands. Despite these modifications, the "proton sponge effect" remains unaffected due to the unmodified secondary and tertiary amines of poly(ethyleneimine). The resulting polymers were pH-sensitive and showed no cytotoxicity in human umbilical vein endothelial cells (HUVEC), suggesting that the primary amines found in PEI are primarily responsible for its cytotoxic effect. With the adhesive peptide RGD as the target ligand, these nanocomplexes were able to facilitate the uptake of siRNA into zebrafish hearts.



## Folic Acid

Most tumor cells (and a subpopulation of macrophages) show an overexpression of folate receptors on their surface. Following fundamental work by Abebe et al.,<sup>9</sup> Mohammadi et al.<sup>14</sup> used folic acid-decorated micelles to target activated macrophages in inflamed joints (Figure 2). The inner core of the micelles consisted of PLLA-PEI-PLLA block copolymers, while the outer layer was prepared with different ratios of PLLA-PEG-PLLA and folic acid (FA)-PEG-PLLA. 75% FA-PEG-PLLA and 25% PLLA-PEG-PLLA were found to be the optimal formulation for effective plasmid DNA encapsulation, cellular uptake, and macrophage targeting. With this composition, a significantly higher GFP expression was achieved in activated RAW 264.7 macrophages *ex vivo*, compared to non-targeting micelles and non-activated macrophages.

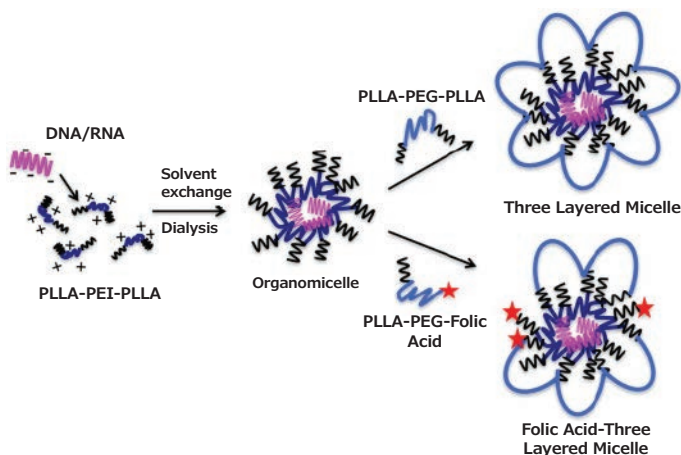


**Figure 2.** Formulation of non-targeted and targeted three-layered micelles in a 2-step process. Depending on the use of PLLA-PEG-PLLA only or blends of PLLA-PEG-PLLA with PLLA-PEG-FA for the outer layer, non-targeted or folate-receptor targeted three-layered micelles are obtained, respectively. Reprinted with permission from Mohammadi et al.<sup>14</sup> Copyright 2016 Elsevier.

## Transferrin

A more established and successful approach towards efficient polyplex shielding, utilizes the highly hydrophilic, negatively-charged serum glycoprotein transferrin (Tf). This ligand combines both an intrinsic stealth effect and targeting towards transferrin-receptor expressing cells,<sup>2</sup> eliminating the need for a PEG-shell to shield the positive charge of the Tf-PEI/DNA complex. This gene delivery system not only exhibits decreased erythrocyte aggregation compared to its PEGylated derivative, but also reduced cytotoxicity (Figure 3). Moreover, the biodistribution pattern was shifted from liver and lung, as typical for unshielded complexes, to transgene expression predominantly in the targeted tumor *in vivo*. Thus, transferrin can be used as a shielding and targeting component, to efficiently deliver genetic material into tumor cells.

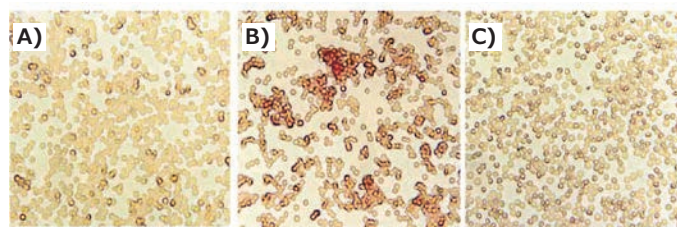


**Figure 3.** Incorporation of transferrin decreases erythrocyte aggregation. Fresh murine erythrocytes were incubated with PEI/DNA or Tf-PEI/PEI/DNA complexes (N/P = 4.8) for 1 h at 37 °C. **A)** Tf-PEI/PEI/DNA, **B)** PEI/DNA, **C)** control. Adapted with permission from Kircheis et al.<sup>2</sup> Copyright 2002 Nature Publishing Group.

## Chemically Modified PEI

Poly(ethyleneimine) has been regarded as the gold standard of polymeric gene carriers due to its high buffering capacity for the endosomal escape of genes, but is severely limited by its high cellular toxicity. The cytotoxicity of PEI depends on its degradability, molecular weight, and structure. In this section, we describe two of the most common linkages incorporated into PEI derivatives to yield degradable analogs.

### Ester Bonds

PEI derivatives containing ester bonds can be prepared by the Michael addition of PEI to diacrylates, which act as crosslinkers. Wang et al.<sup>15</sup> coupled branched, low molecular weight PEI to different Pluronic<sup>®</sup> diacrylates. The poly(ester amine)s (PEA) obtained were examined thoroughly *in vitro* and *in vivo*. PEAs showed limited cytotoxicity toward C2C12 and CHO cells, even in high concentrations, whereas cell viability dropped to less than 15% when using standard PEI (25 kDa). Furthermore, a significant improvement in gene delivery efficacy of CHO, C2C12, and HSkM cells was achieved, as well as effective transfection in mdx mice.

### Disulfide Bonds

The concentration of glutathione and other reducing agents is much higher in the cytoplasm than in the plasma, imparting a high intracellular reduction capacity compared to the extracellular milieu. Redox-sensitive materials typically incorporate degradable disulfide linkages in their backbone, as these bonds degrade in a reducing environment. Cellular uptake with fast intracellular siRNA release *in vitro* was observed when using a disulfide-crosslinked, highly-branched PEI in comparison to unmodified linear and branched PEI.<sup>16</sup> Neu et al.<sup>17</sup> used a low molecular weight crosslinking reagent, dithiobis(succinimidyl propionate) (DSP), to generate crosslinked PEI polyplexes without the additional steric stabilization of hydrophilic copolymers (Figure 4). These polyplexes were comparable in size and DNA condensation properties, and were efficiently taken up by cells *in vitro* with a redox-triggered DNA release. *In vivo* experiments in mice showed increased blood concentrations. A luciferase assay

demonstrated enhanced liver expression and reduced unwanted lung transfection. These results show that DSP-crosslinked PEI creates reducible disulfide bonds that can prolong circulation time and maintain transfection efficiency. Additionally Zhang et al.<sup>18</sup> enhanced DNA delivery and transfection efficiency while reducing cytotoxicity (*in vitro* and *in vivo*) by conjugating a reducible, disulfide-linked PEI to biocompatible Pluronic®.

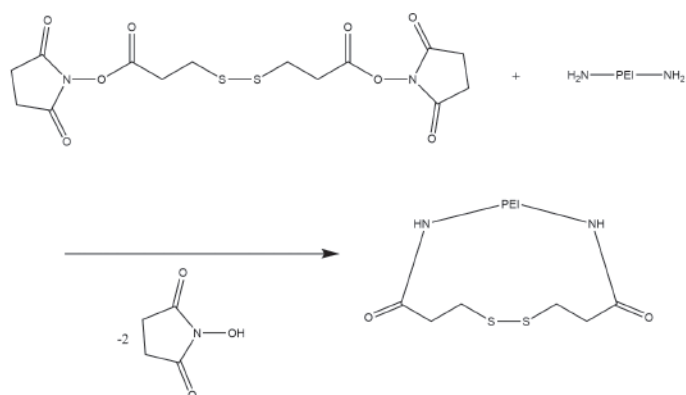


**Figure 4.** Reaction scheme for the conversion of PEI primary amines with dithiobis(succinimidyl propionate) (DSP). The resulting disulfide bonds are easily cleaved by reducing agents.

## Conclusion

As one of the most studied non-viral vectors for nucleic acid delivery, PEI holds significant potential for gene therapy applications. Due to its ability for RNA/DNA condensation, cellular uptake, and endosomal escape, poly(ethyleneimine) is a suitable candidate for the *in vivo* delivery of therapeutic nucleic acids. Although non-modified PEI-based carriers have been considered the gold standard, PEI features several key drawbacks such as cytotoxicity, lack of target specificity, and transfection efficiency. Considerable efforts have been made to assess different modifications of PEI and overcome these drawbacks. Promising results regarding target specificity, transfection efficiency, and biodegradability have been achieved, but there is still significant room for improvement. In the past two decades, substantial advances have been made using degradable PEI-based delivery systems, improving both safety and potency. Scientists have also developed multifunctional polyplexes for receptor-mediated gene delivery *in vivo* (Figure 5),<sup>19</sup> some with the capacity to be used in diagnosis (bioimaging) and therapy, via gene delivery at the same time (theranostics).<sup>20</sup> However, further *in vivo* studies are needed to explore additional pharmacodynamics, pharmacokinetic, and immunogenic properties; improving the potential of PEI-based gene carriers for use in clinical applications.

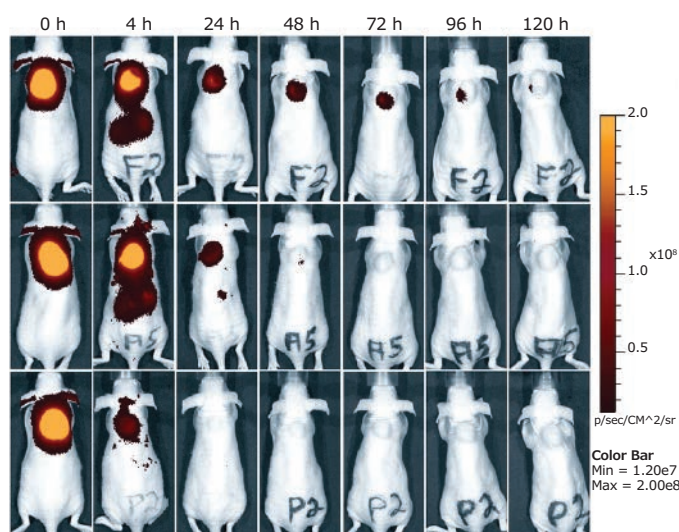


**Figure 5.** Intratumoral injection of siRNA polyplexes. Retention of targeted polyplexes at the tumor site determined by NIR fluorescence bioimaging. Folic acid-targeted polyplexes (top), untargeted polyplexes (center), and equal amounts (25  $\mu$ g) of free Cy7-labeled siRNA (bottom). Adapted with permission of Dohmen et al.<sup>19</sup> Copyright 2012 American Chemical Society

## References

- (1) Boussif, O.; Lezoualc'h, F.; Zanta, M. A.; Mergny, M. D.; Scherman, D.; Demeneix, B.; Behr, J. P. *Proc. Nat. Acad. Sci.* **1995**, *92*(16), 7297-7301.
- (2) Kircheis, R.; Wightman, L.; Schreiber, A.; Robitza, B.; Rössler, V.; Kurs, M.; Wagner, E. *Gene Ther.* **2001**, *8*(1), 28.
- (3) Neu, M.; Germershaus, O.; Behe, M.; Kissel, T. *J. Control. Release* **2007**, *124*(1-2), 69-80.
- (4) Mao, S.; Neu, M.; Germershaus, O.; Merkel, O.; Sitterberg, J.; Bakowsky, U.; Kissel, T. *Bioconjugate Chem.* **2006**, *17*(5), 1209-1218.
- (5) Merkel, O. M.; Beyerle, A.; Librizzi, D.; Pfestroff, A.; Behr, T. M.; Sproat, B.; Barth, P. J.; Kissel, T. *Mol. Pharm.* **2009**, *6*(4), 1246-1260.
- (6) Taranejoo, S.; Chandrasekaran, R.; Cheng, W.; Hourigan, K. *Carbohydr. Polym.* **2016**, *153*, 160-168.
- (7) Gutsch, D.; Appelhans, D.; Höbel, S.; Voit, B.; Aigner, A. *Mol. Pharm.* **2013**, *10*(12), 4666-4675.
- (8) Ndong Ntoutoume, G. M. A.; Grassot, V.; Brégier, F.; Chabanais, J.; Petit, J.-M.; Granet, R.; Sol, V. *Carbohydr. Polym.* **2017**, *164*, 258-267.
- (9) Abebe, D. G.; Kandil, R.; Kraus, T.; Elsayed, M.; Merkel, O. M.; Fujiwara, T. *Macromol. Biosci.* **2015**, *15*(5), 698-711.
- (10) Endres, T.; Zheng, M.; Kiliç, A.; Turowska, A.; Beck-Broichsitter, M.; Renz, H.; Merkel, O. M.; Kissel, T. *Mol. Pharm.* **2014**, *11*(4), 1273-1281.
- (11) Nia, A. H.; Eshghi, H.; Abnous, K.; Ramezani, M. *Eur. J. Pharm. Sci.* **2017**, *100*, 176-186.
- (12) Hu, J.; Zhu, M.; Liu, K.; Fan, H.; Zhao, W.; Mao, Y.; Zhang, Y. *PLOS ONE* **2016**, *11*(12), e0166673.
- (13) Wang, F.; Gao, L.; Meng, L.-Y.; Xie, J.-M.; Xiong, J.-W.; Luo, Y. *ACS Appl. Mater. Interfaces* **2016**, *8*(49), 33529-33538.
- (14) Mohammadi, M.; Li, Y.; Abebe, D. G.; Xie, Y.; Kandil, R.; Kraus, T.; Gomez-Lopez, N.; Fujiwara, T.; Merkel, O. M. *J. Control. Release* **2016**, *244*, 269-279.
- (15) Wang, M.; Wu, B.; Tucker, J. D.; Lu, P.; Lu, Q. *Drug Deliv.* **2016**, *23*(9), 3224-3233.
- (16) Breunig, M.; Hozsa, C.; Lungwitz, U.; Watanabe, K.; Umeda, I.; Kato, H.; Goepferich, A. *J. Control. Release* **2008**, *130*(1), 57-63.
- (17) Neu, M.; Germershaus, O.; Mao, S.; Voigt, K.-H.; Behe, M.; Kissel, T. *J. Control. Release* **2007**, *118*(3), 370-380.
- (18) Zhang, L.; Zhang, Y.; Chen, Z.; He, Y. *Int. J. Nanomedicine* **2016**, *11*, 5245-5256.
- (19) Dohmen, C.; Edinger, D.; Fröhlich, T.; Schreiner, L.; Lächelt, U.; Troiber, C.; Rädler, J. O.; Hadwiger, P.; Vornlocher, H.-P.; Wagner, E. *ACS Nano* **2012**, *6*(6), 5198-5208.
- (20) Wang, M.; Guo, Y.; Yu, M.; Ma, P. X.; Mao, C.; Lei, B. *Acta Biomater.* **2017**, *54*, 69.

## Poly(ethyleneimine)

For a complete list of available materials, visit [SigmaAldrich.com/pei](http://SigmaAldrich.com/pei).

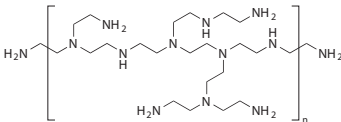
### Linear Poly(ethyleneimine)

Name	Structure	Molecular Weight	Prod. No.
Poly(ethyleneimine), linear		average $M_n$ 2,500	764604-1G
		average $M_n$ 5,000	764582-1G
		average $M_n$ 10,000	765090-1G

### Linear Poly(ethyleneimine) HCl Salt

Name	Structure	Molecular Weight	Prod. No.
Poly(ethyleneimine) hydrochloride		average $M_n$ 4,000	764892-1G 764892-5G
		average $M_n$ 10,000	764647-1G
		average $M_n$ 20,000	764965-1G

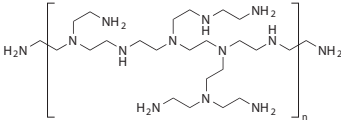
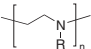
### Branched Poly(ethyleneimine)

Name	Structure	Molecular Weight	Prod. No.
Poly(ethyleneimine), branched		average $M_n$ ~600 by GPC average $M_w$ ~800 by LS	408719-100ML 408719-250ML 408719-1L
		average $M_n$ ~10,000 by GPC average $M_w$ ~25,000 by LS	408727-100ML 408727-250ML 408727-1L

## Poly(ethyleneimine) Solution

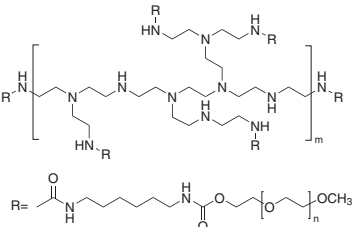
For a complete list of available materials, visit [SigmaAldrich.com/pei](http://SigmaAldrich.com/pei).

### Branched Poly(ethyleneimine)

Name	Structure	Molecular Weight	Concentration	Prod. No.
Poly(ethyleneimine) solution		$M_n$ 600,000-1,000,000	~ 50% in H <sub>2</sub> O	03880-100ML 03880-500ML
		average $M_n$ ~1,200 average $M_w$ ~1300 by LS	50 wt. % in H <sub>2</sub> O	482595-100ML 482595-250ML
		average $M_n$ ~1,800 by GPC average $M_w$ ~2,000 by LS	50 wt. % in H <sub>2</sub> O	408700-5ML 408700-250ML 408700-1L
		average $M_n$ ~60,000 by GPC average $M_w$ ~750,000 by LS	50 wt. % in H <sub>2</sub> O	181978-5G 181978-100G 181978-250G 181978-18KG
		$M_w$ 110,000	37 wt. % in H <sub>2</sub> O	306185-100G 306185-250G
Poly(ethyleneimine), 80% ethoxylated solution	 R = CH <sub>2</sub> CH <sub>2</sub> NR <sub>2</sub> R = H R = CH <sub>2</sub> CH <sub>2</sub> OH			

## Functionalized Poly(ethyleneimine)

For a complete list of available materials, visit [SigmaAldrich.com/pei](http://SigmaAldrich.com/pei).

Name	Structure	Molecular Weight	Prod. No.
Branched PEI-g-PEG		PEG $M_n$ 5,000	900743-1G

# Collagen in Gene Delivery Applications



Morgan A. Urello,<sup>1</sup> Kristi L. Kiick,<sup>2</sup> and Millicent O. Sullivan<sup>1\*</sup>

<sup>1</sup>Dept. of Chemical and Biomolecular Engineering, University of Delaware, Newark DE 19716

<sup>2</sup>Dept. of Material Science and Engineering, University of Delaware, Newark DE 19716

\*Email: msullivan@udel.edu

## Introduction

Collagen-based delivery systems effectively deliver a range of viral and non-viral gene carriers by providing spatiotemporal control over delivery and reducing degradation rates and immune responses. The application of modified collagens has shown significant progress in enhancing bone and tissue repair, slowing tumor growth, and improving the overall efficacy and safety of gene delivery. Modified collagens have also facilitated controlled transgene expression in clinical trials.<sup>1</sup> These advances are enabled by the biocompatibility and versatility of native collagen, which permits the incorporation of genes in collagen-based structures with a diverse range of properties. Furthermore, the development of modified collagens as well as synthetic collagen-mimetic peptides (CMPs) has provided additional control over gene delivery through alteration of vector/collagen affinity, modulation of cell/vector interactions, and increased vector stability.<sup>2,3</sup> Overall, the unique structural properties and bioactivity of collagen and its derivatives coupled with the ease of tailoring its mechanical and degradative properties, and native cellular interactions, make collagen an enormously promising material for engineering high efficiency, tunable gene delivery systems.

## Collagen as a Biomaterial

Collagen is the main structural protein in the extracellular matrix (ECM).<sup>1</sup> It is located throughout skin and other connective tissues, where it provides the mechanical strength and structural integrity necessary for function. The unique shape and structural properties of collagen molecules are determined by their triple-helical  $\alpha$ -domains. The triple helical domains in collagen consist of three polyproline chains composed of multiple triplets with the amino acid sequence Glycine-X-Y (GXY), in which X and Y are most commonly proline and hydroxyproline, respectively. Stabilized primarily by interchain hydrogen bonding the three polyproline chains associate together to produce a tightly packed triple helix.

Collagens play key roles in the cellular adhesion and signaling processes underlying development, tissue repair/regeneration, and cancer.<sup>1</sup> As a biomaterial, collagen can similarly serve as both a bioactive, structural scaffold and a reservoir for retention

and delivery of signaling molecules or genes. Collagen is biodegradable, non-immunogenic, and extremely versatile, and has been used to prepare a wide range of products in various forms. For instance, collagen has been used extensively as an injectable solution that spontaneously gels post-delivery to augment soft tissues, and as a porous, ECM-like sponge for the dressing of wounds.<sup>2</sup>

## Modified Collagens and Collagen-Mimetic Peptides

Of the 28 types of collagen, type I collagen is the most common in nature and in biomaterial applications.<sup>1</sup> Additionally, modified collagens have been developed to enhance collagen biomaterial properties and therapeutic gene delivery applications. Two of the most common collagen-derived biomaterials are atelocollagen and gelatin. Atelocollagen is obtained by pepsin treatment of collagen while gelatin is prepared by thermal denaturation of collagen following acid, alkali, or enzymatic pretreatment. Atelocollagen has similar structural properties to native collagen, yet with reduced immunogenicity due to the removal of the immunogenic telopeptides during enzymatic treatment. Gelatin similarly lacks significant antigenicity and can easily be crosslinked after chemical modification. Uniquely, the processing of gelatin can be used to vary its isoelectric point, which is valuable when forming polyelectrolyte complexes with other polymers or vectors. Additionally, like its collagen precursor, gelatin adheres extremely well to cells; however, intact versus denatured collagens present different integrin-binding sites, leading to significant differences in cell behavior. Alternatively, CMPs have been synthesized with a wide range of properties. These relatively short peptides consist of six to ten GXY triplets and have been engineered with various melting temperatures that can be altered by changing the length and/or composition of the amino acid sequence.<sup>2-4</sup> The peptide's capacity to form a triple helix enables CMP hybridization to native or engineered collagens through a thermal annealing process. The CMP replaces a native collagen chain, typically at locations within the triple helix where the collagen is damaged and more susceptible to strand invasion.

## Collagen-Based Gene Delivery Systems

Collagen has versatile structural properties, which has allowed collagen-based gene delivery systems to be designed in many forms.<sup>1</sup> For instance, solubilized collagen is in a liquid state at cold temperatures but forms a fibrous scaffold at body temperature, permitting pDNA and vectors to be easily

incorporated into collagen while in the liquid state. Subsequently, collagen solutions containing the pDNA or vectors can be fashioned into pellets, sponges, films, gels, beads, etc. without heat processing or use of organic solvents; two key sources of vector deactivation common in other delivery approaches. As summarized in **Figure 1**, each structure has unique benefits.

Structure	Fabrication	Loading	Properties
<b>Bulk/Scaffold-Mediated</b>			
Sponge/Matrix	Freeze-dried collagen gels	Encapsulation pre-freeze-drying	Porous, ECM-like
	Structure dependent on collagen concentration, freeze rate, the size of gel fibers, and presence/absence of crosslinking agent	Immersion in/injection of vector solution typically followed by freeze-drying	Delivery characterized by initial burst release and shorter delivery periods compared to other collagen-delivery strategies  Sustained delivery achieved through crosslinking and vector immobilization/design
Pellet	Commonly fabricated with atelocollagen  Gene/neutralized collagen solutions are injected into a mold and freeze-dried	Encapsulation into collagen precursor solution before gelation and freeze-drying	Small enough to be injected subcutaneously/intramuscularly, yet large enough to remain stationary  Facilitate prolonged delivery without need for chemical treatment  Slow delivery that can be increased through addition of glucose
Hydrogel/Gels	Chemically or physically crosslinked collagen gels fabricated with a range of densities and therapeutic release profiles	Encapsulation into collagen precursor solution  Swelling in vector solution	Swell after hydration with biological fluids and maintain their structural integrity post-soaking  Commonly formulated to enable injection  Tailored delivery achieved through crosslinking and vector immobilization and design
Film	Air-dried collagen solutions/gels	Therapeutic can be encapsulated or bound to the surface either covalently or through non-specific interactions like electrostatics	Coatings with thickness between 0.01-0.5 mm  Sustained delivery through various surface modifications
<b>Nanocarrier-Mediated</b>			
Gelatin-based	Standard protein-based nanoparticle fabrication techniques including emulsification, desolvation, or coacervation	Incorporated into the carrier through physical encapsulation or electrostatic interaction during fabrication	Targeted delivery via surface modification with ligands or by EPR effect for leaky tumors  Cationic carriers electrostatically condense DNA and facilitate cell uptake and endosomal escape
	Solvent choice, temperature, pH, and polymer size used to modulate nanocarrier diameter	Complexation with surface modifying groups after modification	
Cationic Collagens and CMPs	Components electrostatically condense pDNA	Condensed during fabrication	Stabilizes pDNA and facilitates cellular uptake and efficient <i>in vitro</i> transfection

**Figure 1.** Summary of the fabrication, therapeutic loading and properties of common collagen-delivery systems.

subscribe  
today

Don't miss another  
topically focused technical review.

It's **free** to sign up for a print or digital subscription of Material Matters™.

- Advances in cutting-edge materials
- Technical reviews on emerging technology from leading scientists
- Peer-recommended materials with application notes
- Product and service recommendations



MILLIPORE  
SIGMA

To view the library of past issues or to subscribe, visit [SigmaAldrich.com/materialmatters](http://SigmaAldrich.com/materialmatters)

## Collagen Scaffold-Mediated Gene Delivery

Scaffold-mediated delivery has proven to be a promising strategy in overcoming key gene delivery obstacles including off-target effects, immunogenic responses, serum/nuclease instability, and spatiotemporal control. Collagen is a particularly valuable substrate because its diverse structural forms provide different gene delivery profiles, while its similarity to native ECM allows cellular invasion and the corresponding delivery of immobilized genes. Accordingly, over the past two decades, innovative collagen scaffold-based approaches for the delivery of naked pDNA, complexed pDNA, and viral DNA have shown promise in numerous medical applications including bone, wound, cardiac, and optic repair.<sup>1</sup>

### Naked pDNA

The first tissue engineering scaffold to deliver DNA was comprised of collagen and naked pDNA.<sup>5</sup> Naked pDNA delivery represents the simplest form of non-viral vector transfection; however, naked pDNA is not efficiently internalized by cells due to its large size and negatively charged phosphate groups. Naked pDNA also suffers from high susceptibility to nuclease degradation and rapid clearance from the body. Despite these drawbacks, collagen-mediated gene delivery was used in a pioneering study to demonstrate that repair cells (e.g., fibroblasts, chondrocytes, and/or osteoblasts) can be genetically reprogrammed *in vivo* to deliver pDNA encoding osteogenic factors, leading to enhanced bone formation in critically-sized rat femur defects.<sup>5</sup> Specifically, collagen sponge-mediated delivery of naked pDNA encoding bone morphogenetic protein-4 (BMP-4) and parathyroid hormone fragment (PHF) synergistically accelerated the functional union of large segmental defects within four or nine weeks when either one plasmid or both plasmids were delivered, respectively. Delivery from collagen matrices has the potential to immobilize pDNA and increase its local concentration and stability in ways that simple injection of pDNA cannot. Furthermore, more controlled delivery of pDNA from collagen matrices has been achieved by regulating matrix degradation rates through implementing different crosslinking strategies and/or altering the degree of plasmid/matrix integration. Both gene loading efficiency and retention/release profiles have been expanded using physical crosslinking techniques such as dehydrothermal (DHT) and ultraviolet (UV) treatments, and/or chemical methods including 1-ethyl-3-(3-dimethylaminopropyl)carbodiimide (EDC, **Prod. No. E1769**) treatments. For instance, EDC and UV crosslinked collagen-glycosaminoglycan (GSCG) matrices supplemented with luciferase-encoding genes were demonstrated to induce higher transgene expression in chondrocytes over a four week period relative to non-crosslinked and DHT or UV treated matrices.<sup>6</sup> Release from this scaffold was biphasic with an initial burst release period over eight hours followed by a sustained release over the 28-day monitoring period (**Figure 2A**).

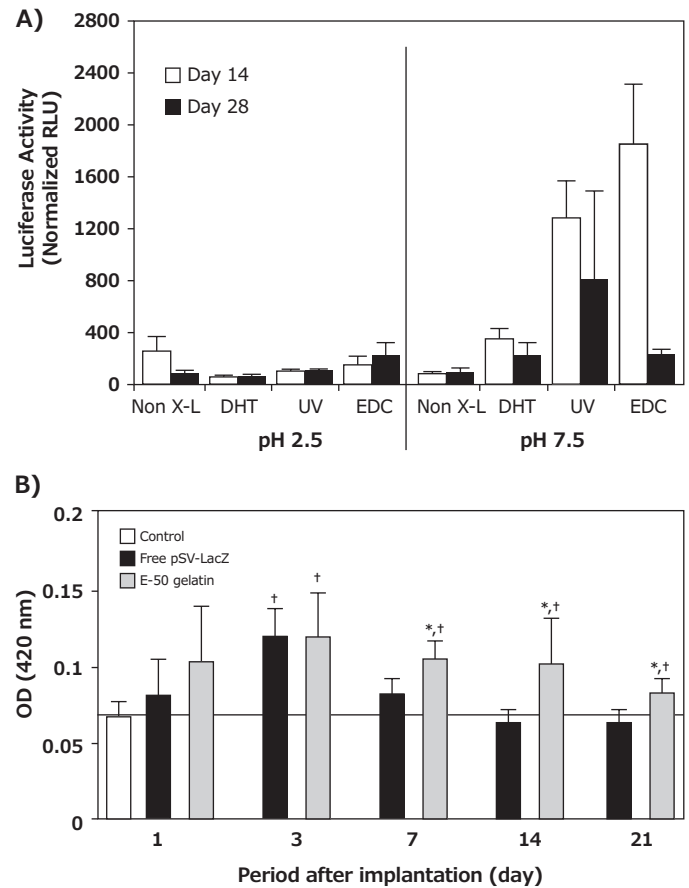


**Figure 2.** Collagen-mediated naked pDNA delivery **A)** Different physical and chemical crosslinking techniques promoted significantly different magnitudes and durations of *in situ* transgene expression within pDNA GSCG matrices encoding luciferase over at 28 day period. **B)** The implantation of cationized gelatin hydrogels incorporating pSV-lacZ into the femoral muscle of mice promoted sustained and higher transgene expression than free pDNA over a 21 day period. Reprinted with permissions from Mary Ann Liebert (Reference 6), copyright (2002) and Elsevier Ltd. (Reference 8), copyright (2003).

Alternatively, sustained, prolonged pDNA delivery from collagen-based hydrogels has been achieved through the utilization of cationized collagen or gelatin, whose altered charge increases pDNA retention by enhancing electrostatic interactions between the scaffold and the pDNA. Cohen-Sacks et al. demonstrated greatly enhanced pDNA retention in poly-L-lysine-modified versus non-modified collagen hydrogels.<sup>7</sup> Moreover, Kushibiki et al. determined that *in vivo* release and gene expression of pDNA could be tailored by preparing crosslinked hydrogels composed of gelatin with different extents of cationization (**Figure 2B**).<sup>8</sup> Significant *in vivo* transgene expression was only reported when the aminized percentage of gelatin was 41 mol% or greater. In contrast, prolonged pDNA delivery has also been obtained in atelocollagen pellets without chemical crosslinking. These injectable, dense pDNA-loaded pellets exhibit sustained, prolonged transgene expression *in vivo* for up to two months compared to three weeks when pDNA was administered alone.<sup>9</sup>

## pDNA Complexes

Most non-viral gene delivery approaches rely on the delivery of complexed pDNA nanoparticles created through the electrostatic assembly of pDNA with cationic polymers or lipids. Complexation has the capacity to improve pDNA serum half-lives through protection from nucleases, and can also facilitate cellular internalization through increased interactions with anionic cell surfaces. Hence, pDNA complexes typically exhibit higher transgene expression efficiencies relative to naked pDNA.<sup>10</sup> Moreover, the use of pDNA complexes offers additional flexibility for regulation of delivery from collagen. Non-specific electrostatic interactions between collagen and gene-loaded carriers, such as lipoplexes and polyplexes, can be tailored through variation of complex charge density and shielding with copolymers to reduce matrix interactions and increase release.<sup>10</sup> For instance, Cohen-Sacks et al. demonstrated complexing pDNA with cationic agents like Lipofectamine™ and poly(ethyleneimine) (PEI) enabled prolonged *in vivo* transgene expression from collagen matrices without the need for linking chemistries or multi-step chemical modification of collagen matrices with cationic polymers.<sup>7</sup> Elangovan et al. prepared collagen matrices loaded with PEI polyplexes encoding

platelet-derived growth factor (PDGF-B). These scaffolds enhanced new bone formation in calvarial defects by 14-fold and 44-fold when compared to empty defects and scaffolds, respectively, when the defects were evaluated at four weeks post-implantation.<sup>11</sup> Vectors have also been engineered with specific affinities for native and modified collagens.<sup>2,12</sup> Segura et al. reported the immobilization of PEI polyplexes onto hyaluronic acid-collagen hydrogels through a combination of non-specific adsorption (electrostatic, hydrophobic, and van der Waals interactions) and biotin/NeutrAvidin® binding. These modified scaffolds increased transgene expression 2-fold after a two day incubation in cultured cells.<sup>12</sup> Urello et al. demonstrated the integration of PEI polyplexes into collagen scaffolds through CMP/collagen hybridization (Figure 3A), with improvements in DNA loading efficiency and serum-stability, as well as coordination of cell-triggered delivery with extra- and intracellular collagen remodeling pathways.<sup>2,3</sup> Moreover, variation in CMP display on the polyplexes enabled tailoring of transgene PDGF-B expression within *in vitro* defect models, which dramatically accelerated wound closure over a 10-day period compared to when collagen containing either low doses of rPDGF-BB or non-modified polyplexes encoding PDGF-B were administered (Figure 3B).

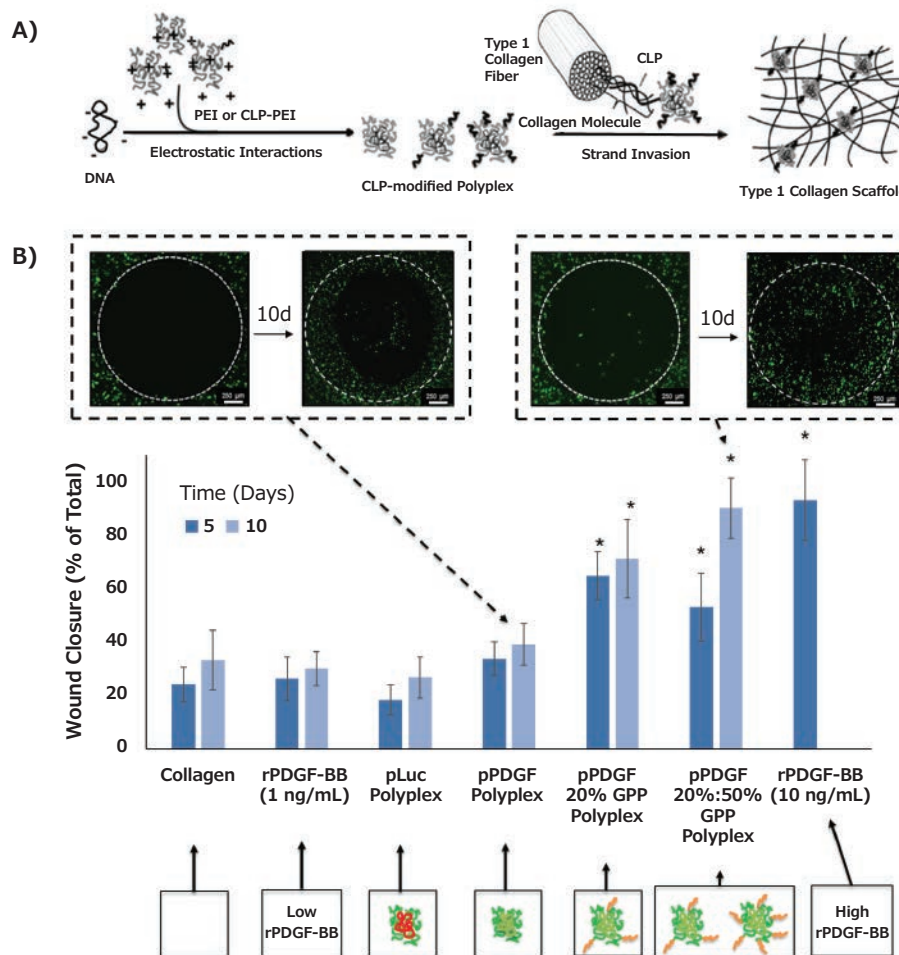


**Figure 3.** Collagen-mediated pDNA complex delivery A) Schematic of DNA/Collagen modification using CMP hybridization. B) CMP display promoted sustained PDGF-BB expression that resulted in >50% increases in % *in vitro* wound closure relative to collagen containing either low doses of rPDGF-BB or non-modified polyplexes encoding PDGF-B within 10 days. Reproduced from Reference 2 with permission from The Royal Society of Chemistry and Reference 3 with permissions.

## Viral Vectors

Viral gene delivery utilizes the innate ability of viruses to transfect cells with high efficiency. One key mechanism underlying the behavior of many viruses is the ability to bind to the ECM, thereby preventing clearance and increasing cellular availability. Accordingly, the delivery of therapeutic viruses from ECM components, such as collagen, has also been extensively studied.<sup>1</sup> Doukas et al. first demonstrated the benefits of biomaterial-mediated viral gene delivery as compared with the direct application of solution formulations of virus or protein-based therapeutics.<sup>13</sup> Specifically, PDGF-B encoding adenovirus formulated in a collagen matrix was shown to significantly enhance healing in rabbit ischemic excisional wounds, whereas repetitive, high dosages of PDGF-BB protein were required to induce neotissue comparable to the single administration of collagen-immobilized AdPDGF-B (Figure 4A). Moreover, the authors demonstrated collagen retained both the vector and transgene products within the wound bed, while the AdPDGF-B vector escaped the wound site when administered in solution and caused PDGF-BB-induced hyperplasia in surrounding tissues. To encourage localized delivery of viral gene carriers, viral vectors have been immobilized onto modified collagens via antibody complexation. Levy et al. first demonstrated successful adenoviral vector delivery based upon anti-adenovirus antibody immobilization within a collagen matrix. Viral vectors were immobilized in type I collagen-avidin gel using a biotinylated, polyclonal antibody specific for the adenovirus hexon. The antibody complexed collagens achieved enhanced, site-specific, efficient gene transfer in both *in vitro* cell studies (compared to non-antibody complexed controls, Figure 4B) and in myocardial injection sites in a pig model (compared to direct vector injections).<sup>14</sup> Antibody-tethered adenovirus delivery was demonstrated to enhance site specific delivery from collagen-coated stents and endovascular microcoils. Alternatively, viruses have been encapsulated into nanocarriers to enhance stability and prevent vector escape from collagen hydrogels. Shin and Shea demonstrated lentivirus-loaded, hydroxyapatite nanoparticles promoted retention in low density collagen hydrogels, were conducive to cell invasion, and promoted overall higher levels of expression in subcutaneous mouse implants over a four day monitoring period.<sup>15</sup> When the vector is completely immobilized within the biomaterial, vector uptake is reliant on cellular invasion; therefore, the capacity of collagen to facilitate cellular adhesion, proliferation, and migration make it an ideal gene delivery system.

### A)

Treatment	Granulation fill (%)	Protein (mg/sponge)	DNA (µg/sponge)
0.15% Collagen vehicle	28 ± 13	16 ± 2	103 ± 22
AdPDGF-B	81 ± 15 <sup>a</sup>	30 ± 6 <sup>a</sup>	218 ± 28 <sup>a</sup>
PDGF-BB, 100 µg	64 ± 12 <sup>b</sup>	22 ± 4 <sup>b</sup>	155 ± 26 <sup>b</sup>
PDGF-BB, 10 µg <i>qod</i> x 3 <sup>c</sup>	77 ± 9 <sup>b</sup>	31 ± 8 <sup>a</sup>	230 ± 75 <sup>a</sup>

PVA sponges implanted in rats were injected with either 0.15% collagen vehicle or collagen containing AdPDGF-B. Alternatively, PDGF-BB protein was delivered as a single 100 µg dose on day 4 postimplantation, or as 10 µg doses on days 4, 6, and 8. Sponges were removed on day 12 postimplantation and processed to determine the percent granulation fill as well as total protein and DNA contents. Data are presented as means ± SD (*n* = 4–8).

<sup>a</sup>*p* < 0.0001 versus collagen control and *p* < 0.05 versus 100 µg PDGF-BB.

<sup>b</sup>*p* < 0.03 versus collagen control.

<sup>c</sup>*qod* x 3, every other day, three times.

### B)

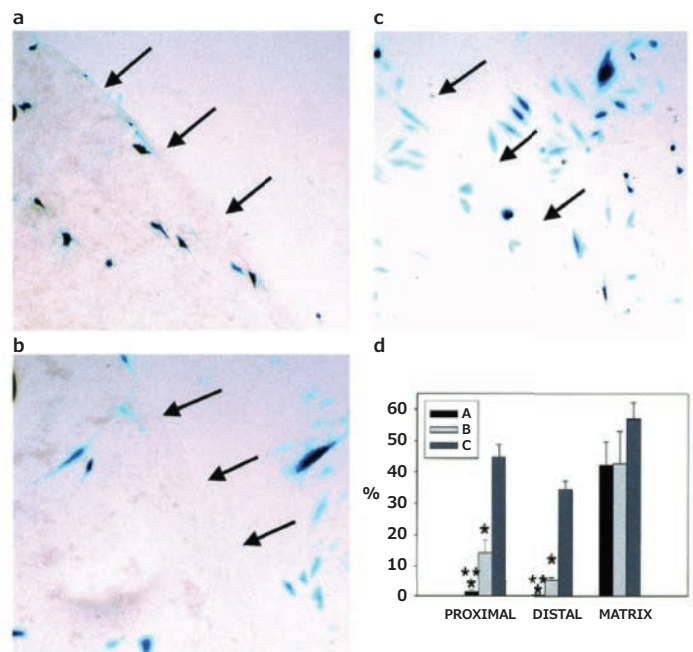


**Figure 4.** Collagen-mediated viral vector delivery. **A)** PDGF-B encoding adenovirus (AdPDGF-B) loaded PVA-collagen sponges in a rabbit ischemic wound model facilitated a 53% increase in granulation tissue relative to an empty sponge and repetitive dosages of PDGF-BB was required to achieve a comparable effect. **B)** Antibody-complexed adenovirus within a collagen-NeutrAvidin<sup>®</sup> promoted transgene  $\beta$ -galactosidase expression localized to the matrix as indicated in the representative images, where the arrows indicate the edge of the collagen matrix. **(a)** Complexed-adenovirus; **(b)** Non-complexed adenovirus; **(c)** No supplement. **(d)** The percentage of transfectant rat arterial smooth muscle cells expressing  $\beta$ -galactosidase in the matrix, distal (within 100 mm) to the matrix, and proximal (>100 mm) from the matrix. Reprinted with permission from Mary Ann Liebert (Reference 13), copyright (2001), and Macmillan Publishers Ltd: Gene Therapy (Reference 14), copyright (2001).



## Collagen Nanocarriers/Microcarriers

Gene-loaded collagen nano-/microcarriers, with collagen as the nano-/microparticle forming agent, represent an alternative to traditional complexation agents and provide a means to form injectable, systemic, and controlled-release systems. Due to the ease of controlling particle size, large surface area, high adsorption capacity, and dispersion ability in water, collagen nanocarriers have been utilized for the sustained release of multiple drugs. Collagen-based nanocarriers have also been shown to prolong circulation time, reduce immunogenic responses, and trigger high levels of cellular uptake. Moreover, collagen-based nanocarriers can be modified with moieties to stimulate targeted delivery and receptor-mediated endocytosis, are able to incorporate multiple plasmids, and can preserve pDNA bioactivity by preventing nuclease degradation. While collagen can form gels without chemical crosslinking, chemical treatments are required to create stable collagen nanoparticles. Wang et al. demonstrated that methylated collagen, DNA carriers were stable at neutral pH and had higher transfection efficiencies *in vitro* compared to pDNA alone or chemically unstable collagen DNA carriers; however, these findings did not translate *in vivo*.<sup>16</sup>

Gelatin has been thoroughly studied as a potential material for colloidal carrier systems. In solution, gelatin undergoes a coil-helix transition followed by aggregation driven by the formation of collagen-like triple helices to enable nanoparticle formation. Additionally, gelatin contains a high number of functional groups that can be used for chemical modification, including crosslinking and functionalization with additional ligands.<sup>1</sup> pDNA can be incorporated into gelatin nanocarriers through physical encapsulation, electrostatic interactions, or complexation with surface modifying groups. For instance, negatively-charged type B gelatin was used to physically encapsulate pDNA (at neutral pH) and the resulting hydrogel-like nanocarriers were demonstrated to successfully accumulate within tumors in murine lung and breast cancer models.<sup>17</sup> Kommareddy et al. proposed these effects were driven by the enhanced permeability and retention (EPR) effect and the incorporation of a poly(ethylene glycol) (PEG) shielding layer which prolonged systemic circulation time (Figure 5). Alternatively, type A gelatin can electrostatically complex DNA (at pH values below 5) to form coacervate particles, and these particles can then be crosslinked to create physiologically-stable carriers. Crosslinked type A gelatin nanocarriers have exhibited *in vitro* transfection efficiencies comparable to the commercial transfection agent

Lipofectamine.<sup>18,19</sup> Moreover, intramuscular injection of these nanocarriers facilitated higher and more sustained transgene expression, in comparison to naked pDNA or Lipofectamine-pDNA complexes over 21 days.<sup>18,19</sup> Cationized gelatin nanocarriers also have been prepared via the modification of gelatin carboxyl groups with amine residues through reaction with cholamine, poly(ethyleneimine), or ethylenediamine. In numerous studies, these particles have been demonstrated to efficiently condense and protect pDNA, promote cellular uptake via interaction with anionic cell membranes, induce endosomal/lysosomal escape through the “proton sponge” effect, and facilitate high levels of transgene expression with low cytotoxicity.<sup>19</sup> For additional information, gelatin-based nanocarriers and their applications in drug and gene delivery have been extensively reviewed by Elzoghby.<sup>19</sup>

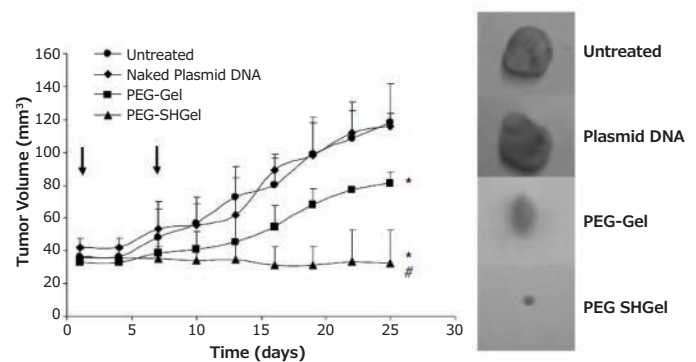


**Figure 5.** Highlighted nanocarrier example, thiolated and non-thiolated PEGylated type B gelatin nanocarriers loaded with pDNA encoding an anti-angiogenic agent stopped tumor growth for 20 days after intravenous administration in mice bearing orthotopic MDA-MB-435 breast adenocarcinoma xenografts. Reprinted with permission from Macmillan Publishers Ltd: Gene Therapy (Reference 17), copyright (2007).

## Conclusions and Outlook

The innate cell adhesive and versatile nature of collagen make it an ideal material for gene delivery applications. Variations in the composition and design of collagen-based carriers and vectors have been used to achieve sustained transgene expression in multiple *in vivo* models (Figure 6), leading to improvements in bone and tissue repair, tumor targeting, and enhancements in overall gene delivery efficiency, compared with alternative delivery systems. Several key strategies should be considered to further expand the utility of collagen in gene delivery.

Vector	Material/ Method	Species/ Location	Gene	Result	References
<b>pDNA</b>					
Plasmid	Collagen Sponge/ Adsorption	Rat/Femur	<i>BMP-4, PHF</i>	Synergistic bone formation	5
Plasmid	Atelocollagen Mini-Pellet/ Encapsulation	Mouse/ Intramuscular Injection	<i>FGF-4</i>	Increase in platelets 2 months	9
<b>pDNA Complexes</b>					
Poly-D-lysine/Plasmid	Collagen Matrix/Adsorption	Rat/Optic Nerve	<i>FGF-2, NT3, BDNF</i>	Sustained neuron survival	21
Poly(ethyleneimine)/Plasmid	Collagen Matrix/Adsorption	Rat/Femur	<i>PDGF-B</i>	Bone formation	11
CMP Poly(ethyleneimine)/ Poly(ethyleneimine) Plasmid	Collagen Gel/Encapsulation and Triple Helix Hybridization	<i>In Vitro/Defect Model</i>	<i>PDGF-B</i>	Accelerated wound closure over a 10-day period	3
<b>Viral Vectors</b>					
Adenovirus	Collagen Gel/Encapsulation	Rabbit/Ischemic Dermal Wound	<i>PDGF-B, FGF-2, VEGF</i>	Enhances granulation tissue, vascularization, and wound closure	13
Adenovirus	Antibody-Modified Collagen Gel/Antigen-Antibody	Pig/ Myocardial Injection	<i>GFP</i>	Localized transgene expression	14
Lentivirus	Collagen Gel/Loaded in Encapsulated Hydroxyapatite Nanoparticles	Mouse/ Subcutaneous Implant	<i>Luciferase</i>	Enhanced lentivirus stability and localized transgenes expression	15
<b>Nanocarriers</b>					
Type B Gelatin/Plasmid	Aqueous/PEGylated, Thiolated Gelatin Nanocarrier	Mouse/Intravenous	<i>Anti-angiogenic sFlt-1</i>	Suppression of tumor growth for 25 days	17
Type A Gelatin/Plasmid	Aqueous/Cationic Nanocarrier	Mouse/ Intramuscular	<i>β-gal</i>	Enhanced expression for 21 days	19

**Figure 6.** Highlighted collagen gene delivery studies in delivery/healing models using a variety of approaches and vectors.

### Methods to Improve Intracellular Trafficking

Non-viral delivery strategies must address intracellular trafficking obstacles to obtain transfection comparable to viral vectors. In collagen-based delivery approaches, trafficking has been directed to high efficiency pathways through the inclusion of integrin-targeted peptides, facilitating specific endocytic uptake. Such approaches could be further tailored through the incorporation of nuclear proteins and peptides to enhance nuclear uptake/retention.<sup>20</sup>

### Delivery from Collagen-Based Gels with Better Controlled Properties

The replacement of collagen with CMPs offers great potential in gene delivery, as the CMP sequence and properties are engineered for specific applications. Compared to collagen, CMPs offer additional tailorability, lower antigenicity, and enhanced stability. A diverse array of thermosensitive, self-assembling carriers, and hydrogels have been fabricated utilizing CMPs,<sup>4</sup> and the application of these structures in gene delivery has the potential to enable efficient, responsive delivery.<sup>2,3</sup>

### Approaches to Achieve Tailored, Multi-Gene Expression

In applications such as wound healing, multiple therapeutic agents must operate synergistically; this makes sequential and co-delivered gene delivery approaches beneficial. Multi-agent delivery has been achieved using layer-by-layer films, encapsulation of therapeutic-loaded nanocarriers, use of additional agents within scaffolds, and engineering different agent/substrate affinities for diverse release profiles.<sup>1-3,7</sup> While these strategies have been explored for small molecule drug and protein therapy, few studies have utilized these approaches for gene delivery.

Given the prevalence of collagen within the body and its importance in determining healthy versus diseased states in tissue, collagen-based gene delivery approaches will continue to improve as our knowledge of biological systems and material science progresses.<sup>21</sup>

## References

- (1) Malafaya, P. B.; Silva, G. A.; Reis, R. L. *Adv. Drug Deliv. Rev.* **2007**, *59*, 207-233.
- (2) Urello, M. A.; Kiick, K. L.; Sullivan, M. O. *J. Mater. Chem. B* **2014**, *2*, 8174-8185.
- (3) Urello, M. A.; Kiick, K. L.; Sullivan, M. O. *Bioengineering & Translational Medicine* **2016**, *1*, 207-219.
- (41) Luo, T. Z.; Kiick, K. L. *Bioconjugate Chem.* **2017**, *28*(3), 816-827.
- (5) Fang, J. M.; Zhu, Y. Y.; Smiley, E.; Bonadio, J.; Rouleau, J. P.; Goldstein, S. A.; McCauley, L. K.; Davidson, B. L.; Roessler, B. J. *Proc. Natl. Acad. Sci. U.S.A.* **1996**, *93*, 5753-5758.
- (6) Samuel, R. E.; Lee, C. R.; Ghivizzani, S. C.; Evans, C. H.; Yannas, I. V.; Olsen, B. R.; Spector, M. *Hum. Gene Ther.* **2002**, *13*, 791-802.
- (7) Cohen-Sacks, H.; Elazar, V.; Gao, J. C.; Golomb, A.; Adwan, H.; Korchov, N.; Levy, R. J.; Berger, M. R.; Golomb, G. J. *Control. Release* **2004**, *95*, 309-320.
- (8) Kushibiki, T.; Tomoshige, R.; Fukunaka, Y.; Kakemi, M.; Tabata, Y. *J. Control. Release* **2003**, *90*, 207-216.
- (9) Ochiya, T.; Takahama, Y.; Nagahara, S.; Sumita, Y.; Hisada, A.; Itoh, H.; Nagai, Y.; Terada, M. *Nat. Med.* **1999**, *5*, 707-710.
- (10) Scherer, F.; Schillinger, U.; Putz, U.; Stemberger, A.; Plank, C. J. *Gene Med.* **2002**, *4*, 634-643.
- (11) Elangovan, S.; D'Mello, S. R.; Hong, L.; Ross, R. D.; Allamargot, C.; Dawson, D. V.; Stanford, C. M.; Johnson, G. K.; Sumner, D. R.; Salem, A. K. *Biomaterials* **2014**, *35*, 737-747.
- (12) Segura, T.; Chung, P. H.; Shea, L. D. *Biomaterials* **2005**, *26*, 1575-1584.
- (14) Doukas, J.; Chandler, L. A.; Gonzalez, A. M.; Gu, D. L.; Hoganson, D. K.; Ma, C. L.; Nguyen, T.; Printz, M. A.; Nesbit, M.; Herlyn, M.; Crombleholme, T. M.; Aukerman, S. L.; Sosnowski, B. A.; Pierce, G. F. *Hum. Gene Ther.* **2001**, *12*, 783-798.
- (15) Levy, R. J.; Song, C.; Tallafragada, S.; DeFelice, S.; Hinson, J. T.; Vyavahare, N.; Connolly, J.; Ryan, K.; Li, Q. *Gene Ther.* **2001**, *8*(9), 659-667.
- (16) Shin, S.; Shea, L. D. *Mol. Ther.* **2010**, *18*, 700-706.
- (17) Wang, J.; Lee, I. L.; Lim, W. S.; Chia, S. M.; Yu, H.; Leong, K. W.; Mao, H. Q. *Int. J. Pharm.* **2004**, *279*, 115-126.
- (18) Kommareddy, S.; Amiji, M. *Cancer Gene Ther.* **2007**, *14*, 488-498.
- (19) Leong, K. W.; Mao, H. Q.; Truong-Le, V. L.; Roy, K.; Walsh, S. M.; August, J. T. *J. Control. Release* **1998**, *53*(1-3), 183-193.
- (20) Elzoghby, A. O. *J. Control. Release* **2013**, *172*, 1075-1091.
- (21) Munsell, E. V.; Ross, N. L.; Sullivan, M. O. *Curr. Pharm. Des.* **2016**, *22*, 1227-1244.
- (22) Berry, M.; Gonzalez, A. M.; Clarke, W.; Greenlees, L.; Barrett, L.; Tsang, W.; Seymour, L.; Bonadio, J.; Logan, A.; Baird, A. *Mol. Cell. Neurosci.* **2001**, *17*, 706-716.

## High-Purity Collagen

For a complete list of available materials, visit [SigmaAldrich.com/hpcollagen](http://SigmaAldrich.com/hpcollagen).

Name	Concentration	Endotoxin (EU/mL)	Prod. No.
Bovine Collagen Solution, Type I sterile filtered, BSE-Free, suitable for biomedical research	6 mg/mL	< 1.0	804622-20ML
Bovine Collagen Solution, Type I sterile filtered, BSE-Free, suitable for biomedical research	3 mg/mL	< 0.5	804592-20ML
Bovine Collagen Solution, Acid soluble telocollagen, Type I sterile filtered, BSE-Free, suitable for biomedical research	6 mg/mL	< 10	804614-20ML
Bovine Tendon Powder, long fiber, Type I collagen, ≥ 60% collagen, suitable for biomedical research	-	< 10	900722-1G
Bovine Tendon Powder, neutral, Type I collagen, suitable for biomedical research	-	< 20	900723-1G
Bovine Fibrillar Collagen Solution, Type I, 65 mg/mL, pH 7.0, suitable for biomedical research	65 mg/mL	< 0.25	900721-1ML

**Sigma-Aldrich**<sup>®</sup>  
Lab Materials & Supplies

**Chemical** SOLUTIONS TO  
**Biological** PROBLEMS

## Bring science together.

Innovators are often misunderstood. But with elite chemical biology products and expertise from MilliporeSigma, you can break through the barrier between disciplines and help lead the scientific community into an emerging field.

## Sigma-Aldrich Chemical Biology

Bioconjugation | Peptide Synthesis | Chemical Probes & Tools

[SigmaAldrich.com/chemicalbiology](http://SigmaAldrich.com/chemicalbiology)

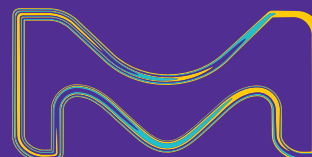
**Millipore**  
**SIGMA**

The life science business of Merck KGaA, Darmstadt, Germany operates as MilliporeSigma in the U.S. and Canada.



# Excellence in Multiferroics

**Dr. Nicola Spaldin Named  
2017 Materials Research Society  
Mid-Career Researcher**



The Materials Research Society (MRS) has chosen Nicola Spaldin, Swiss Federal Institute of Technology, Zürich (ETH Zürich) to receive the Mid-Career Researcher Award both for her new theoretical framework describing multiferroics and for her service to the materials community. Spaldin will be recognized during an awards ceremony at the 2017 MRS Spring Meeting in Phoenix and will deliver her presentation at the 2017 MRS Fall Meeting in Boston. The Mid-Career Researcher Award is endowed by the life science business of Merck KGaA, Darmstadt, Germany, which operates as MilliporeSigma in the U.S. and Canada.

## About Dr. Spaldin

Spaldin holds the chair for Materials Theory at ETH Zürich, where her research group studies the fundamentals of strongly correlated materials. Her work combines the development of new theoretical electronic structure techniques, the study of unusual behavior in existing materials, and the design and synthesis of new materials. Spaldin is particularly renowned for her development of multiferroic materials, that combine simultaneous ferromagnetism and ferroelectricity—and for exploring their application in areas ranging from device physics to cosmology.